A Critical Review of the Stress Corrosion Cracking (SCC) of Magnesium Alloys

ARTICLE *in* ADVANCED ENGINEERING MATERIALS · AUGUST 2005

Impact Factor: 1.76 · DOI: 10.1002/adem.200500071

8 AUTHORS, INCLUDING:

Andrej Atrens
University of Queensland
291 PUBLICATIONS **9,118** CITATIONS
SEE PROFILE

Guang-Ling Song
Oak Ridge National Laboratory
191 PUBLICATIONS **8,385** CITATIONS
SEE PROFILE

Karl Ulrich Kainer
Helmholtz-Zentrum Geesthacht
446 PUBLICATIONS **5,595** CITATIONS
SEE PROFILE

Norbert Hort
Helmholtz-Zentrum Geesthacht
281 PUBLICATIONS **3,395** CITATIONS
SEE PROFILE

A Critical Review of the Stress Corrosion Cracking (SCC) of Magnesium Alloys**

By *Nicholas Winzer**, *Andrej Atrens*, *Guangling Song*, *Edward Ghali*, *Wolfgang Dietzel*, *Karl Ulrich Kainer*, *Norbert Hort* and *Carsten Blawert*

This review aims to provide a foundation for the safe and effective use of magnesium (Mg) alloys, including practical guidelines for the service use of Mg alloys in the atmosphere and/or in contact with aqueous solutions. This is to provide support for the rapidly increasing use of Mg in industrial applications, particularly in the automobile industry. These guidelines should be firmly based on a critical analysis of our knowledge of SCC based on (1) service experience, (2) laboratory testing and (3) understanding of the mechanism of SCC, as well as based on an understanding of the Mg corrosion mechanism.

1. Introduction

1.1. Mg Alloys

Magnesium (Mg) is the most reactive engineering material, and consequently corrosion protection is an issue of great importance[1–4] particularly for its greatest single market, the automobile industry[5] where there has been a 20 % annual growth over the last 10 years, so that the 2002 annual use in North America is ~58,000 tonnes. The total annual Mg usage is 415,000 tonnes; in 2002 primary metal shipments were 364,959tonnes.[6] The rapid increase is due to the lightweight and consequently the favourable strength-to-weight ratio of Mg alloys, which provides considerable weight saving potential in automobile and transport industries. Its good processing capabilities, particularly its ability to be die cast into large thin sections, can also lead to considerable economic savings. Castings are more popular than wrought material because the hexagonal structure of Mg alloys provides challenges to the mechanical processing of wrought alloys, particularly cold working.

Song and Atrens,[1,2] Ghali[3] and Ghali et al.[7,8] have reviewed the corrosion of Mg alloys, and there is much useful information in the ASM handbook[9] and the book by Polmear.[10] The poor corrosion resistance of Mg alloys in aqueous solutions results from (1) the high intrinsic dissolution tendency of Mg, which is only weakly inhibited by corrosion product films, and (2) the presence of impurities and second phases acting as local cathodes and thus causing local galvanic acceleration of corrosion.

[*] *N. Winzer, Prof. A. Atrens, Dr. G. Song*
Materials Division, School of Engineering
The University of Queensland
Brisbane, Qld Australia 4072
Prof. E. Ghali
Department of Mining
Metallurgical and Materials Engineering
Laval University
Quebec, Canada, G1K 7P4
Dr. W. Dietzel, Prof. K. U. Kainer, Dr. N. Hort, Dr. C. Blawert
Institute for Materials Reseach
GKSS-Forschungszentrum Geesthacht GmbH
D-21502 Geesthacht, Germany

[**] *This research was supported by an Australian Research Council (ARC) Linkage grant in collaboration with General Motors Corporation USA. Atrens and Ghali wish to thank GKSS-Forschungszentrum Geesthacht GmbH for their considerable support that allowed them to work at GKSS as visiting scientists.*

1.2. Stress Corrosion Cracking (SCC)

Stress Corrosion Cracking (SCC)[11,12] is a particularly dangerous and complicated form of corrosion. SCC involves a three-way interaction: (1) mechanical loading providing a stress, (2) a susceptible alloy and (3) an environment, often one in which there is an acceptable rate of general corrosion. SCC is related to hydrogen embrittlement (HE). For HE, the environment is hydrogen (*H*), which can be in gaseous form, or can be liberated at the alloy surface by corrosion, or the source of the *H* can be internal, contained inside the alloy from prior processing. *H* is also often postulated to be involved in the mechanism by which SCC initiates and propagates.

SCC is an extremely dangerous type of corrosion damage in engineering service of plant and equipment. Under mechanical loading conditions otherwise considered to be safe, SCC causes slow, sub-critical crack growth. When the critical crack size is reached, the combination of the crack plus the applied load causes sudden, catastrophic fast fracture.

Commonly, it is considered[11–13] that the following three parameters can be used to characterise the SCC of a particular alloy/environment combination: the threshold stress, σ_{SCC}, the threshold stress intensity factor, K_{1SCC}, and the steady state stress corrosion crack velocity. These parameters are explained in more detail in Section 3.2.

Mechanistically, SCC is quite subtle and there is no SCC system where there is complete mechanistic understanding. At best, there are systems where there are good models to describe certain aspects of the whole picture. Thus, it is possible to have separate mechanistic models for different aspects of SCC. Furthermore, a mechanistic model to allow understanding of the environmental influences may concentrate on aspects different to those important in the mechanistic understanding of SCC propagation.

SCC is generally attributed to one of two groups of mechanism: anodic dissolution or cleavage. Only a brief introduction is provided here; Section 4 provides a more complete discussion. For the dissolution mechanism, in its simplest form, dissolution at a film-free crack tip causes crack advance, as illustrated in Figure 1. Figure 2 illustrates a cleavage type mechanism: (1) an embrittled region forms ahead of the crack tip, (2) a crack propagates through the embrittled region, and (3) the crack is stopped as it enters the ductile parent material. The cleavage process recurs once there is again an embrittled region ahead of the crack tip.

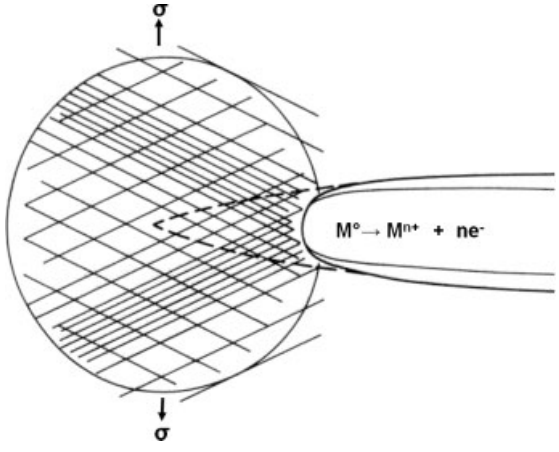

Fig. 1. Continuous crack propagation by dissolution following film rupture. [13]

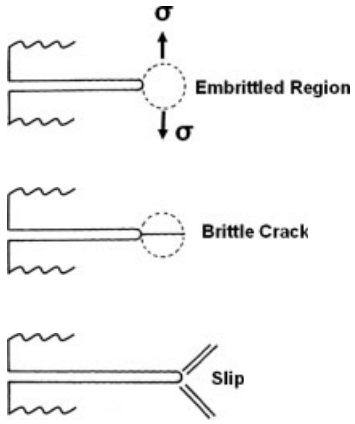

Fig. 2. Model for transgranular cracking in Mg-Al alloys. [14]

SCC is a particular form of environment-assisted cracking which is the more-general term that can include corrosion fatigue. It is obvious that corrosion fatigue (CF) can be important in many service conditions. For example, CF can help in the initiation of the fracture whilst SCC could assist in the propagation of CF. Furthermore, slow cyclic loading has been shown to be important in the initiation of SCC in pipeline steels, and ripple loading may also decrease the SCC thresholds for Mg alloys. However, a consideration of CF of Mg alloys is outside the scope of this review.

1.3. Industrial Context

Mg alloys are known to be susceptible to SCC, particularly in laboratory tests, but it has been proposed that the pre 1980s service failures have been rare and have usually resulted from residual stresses.[15,16] This includes (1) airplane panels examined by Dow, (2) the failures of a number of forged AZ80 French aircraft components, apparently resulting from excessive assembly and residual stresses, and (3) service failures of cast and forged South African Mg aircraft wheels. Speidel,[17] in a comprehensive review of more than 3000 unclassified failure reports from aerospace companies, government agencies, and research laboratories in the United States and five Western European countries, estimated that approximately 10 to 60 Mg aerospace component SCC service failures occurred each year from 1960 to 1970. Of this total, more than 70 % involved either the cast alloy AZ91-T6 or the wrought alloy AZ80-F. Unpublished work by MEL, and confidential industrial reports from the USA, indicate some incidents of SCC for Zr containing alloys.[18] Moreover, the

section of the authoritative ASM Handbook,[9] Vol 13, "Corrosion" on SCC of Mg alloys can be summarised as follows. Mg alloys containing more than 1.5 % Al are susceptible to SCC. Wrought alloys appear more susceptible than cast alloys. Whilst there is little documentation of service SCC of castings, laboratory tests can cause SCC at tensile loads less than 50 % of yield stress in environments causing negligible corrosion. The low incidence of service SCC failures can be attributable to low actual stresses[9] applied in service *in the past*.

However, the incidence of SCC may be expected to increase because Mg parts are now increasingly used in structural applications compared with the non-structural applications in the past. This means that the service conditions for Mg alloys are rapidly becoming more severe, particularly in the automobile industry where cast Mg components are being increasingly used in load-bearing applications. The increasing use of Mg is being facilitated by improvements in casting technology, so that the cost of cast Mg components is very attractive. Automobile examples include: engine blocks, transmission housings, engine oil pans, wheels, and structural body castings such as doorframes, body connectors and cross-members.[19] Moreover, humid air is no longer the only environment that is of concern in causing SCC. Aqueous solutions must also be considered in the automotive applications enunciated above.

Increased SCC incidence may be expected because of the increased loads. Increased loading is a natural progression as designers decrease the section sizes of components as part of the environmental imperative to decrease weight. Moreover, the Mg components in the load bearing applications are increasing in complexity, and this increasing complexity increases the probability of high loads in some parts of such components. Galvanic, localized, or intergranular corrosion, and even thinning by uniform corrosion, could initiate SCC.

1.4. Aims of the Review

The purpose of this paper is to provide a critical review of the literature on SCC. This review builds on the prior reviews, our understanding of the Mg corrosion mechanism,[1,2,3,20–35] SCC,[11,12,36–51] HE,[52–55] (corrosion) fatigue,[56,57] diffusion[58] and passivity.[59–61] Our aim is to provide a foundation for the safe and effective use of Mg and to provide support for the rapidly increasing use of Mg in industrial applications, particularly in automobiles. Thus, the paper aims to provide guidelines to the practical use of Mg. The guidelines should be firmly based on a critical analysis of our knowledge of SCC based on (1) service experience, (2) laboratory testing and (3) understanding of the mechanism of SCC as well as based on an understanding of the Mg corrosion mechanism.

2. Corrosion Mechanism

This section summarises those aspects of the Mg corrosion mechanism[2] of most importance to understanding the SCC of Mg. Corrosion of Mg occurs at breaks in a partially protective surface film. Hydrogen (H) evolution is intimately associated with Mg dissolution in two separate ways. (a) An electrochemical reaction, Equation 1, balances the Mg dissolution reaction, Equation 2. (b) H is also produced directly by the reaction of Mg^+ with water, Equation 3. Note that the overall reaction, Equation 4, produces one molecule of H gas for each atom of Mg dissolved. Furthermore, the overall reaction consumes H^+ and produces OH^-, i.e., the pH increases, which favours the formation of Mg hydroxide film by the precipitation reaction, Equation 5. In steady state, the overall reaction is given by Equation 6.

$$2H^+ + 2e = H_2 \quad \textit{(cathodic partial reaction)} \quad (1)$$

$$2Mg = 2Mg^+ + e \quad \textit{(anodic partial reaction)} \quad (2)$$

$$2Mg^+ + 2H_2O = 2Mg^{++} + 2OH^- + H_2 \quad \textit{(chemical reaction)} \quad (3)$$

$$2Mg + 2H^+ + 2H_2O = 2Mg^{++} + 2OH^- + 2H_2 \quad \textit{(overall reaction)} \quad (4)$$

$$Mg^{2+} + 2OH^- = Mg(OH)_2 \quad \textit{(product formation)} \quad (5)$$

$$Mg + 2H_2O = Mg(OH)_2 + H_2 \quad \textit{(overall reaction in steady state)} \quad (6)$$

2.1. Negative Difference Effect (NDE)

Mg has an exceedingly strange phenomenon, the negative difference effect (NDE). Song, Atrens et al.,[2,62] have provided a comprehensive analysis. As discussed in Section 1.2, H is often postulated to be involved in the mechanism of SCC. Because of the NDE, anodic polarisation causes an increased amount of H evolution on Mg, whereas, there can be a lower amount of H evolved during cathodic polarisation. Implications are further explored in Section 4 on SCC propagation mechanisms.

It is useful to also consider the H fugacity, f_H. If it is assumed that Equation 1 is in equilibrium on a metal surface at a potential E, in a solution of a particular pH value, then the Nernst equation[63,64] provides an estimate of the H fugacity, f_H. The Nernst equation can be written in the following form:

$$f_H = k_1 \exp(k_2[E_H - E]) \quad (7)$$

where k_1 and k_2 are constants. E_H is the reference equilibrium potential of the H evolution reaction, and is equal to the

standard potential for a solution with pH = 0 and with $f_H = 1$ atmosphere. The constant k_1 is determined by the fact that $f_H = 1$ atmosphere when $[E_H - E] = 0$. Equation 7 can be used to estimate the equilibrium hydrogen fugacity at the surface of Mg freely corroding in an aqueous solution, if the numerical value of the free corrosion potential is substituted into Equation 7. The equilibrium *H* fugacity, f_H, so estimated is extremely large because the quantity $[E_H - E]$ is large, over 1000 mV. Thus the *H* fugacity (estimated from Eq. 7) at the surface of Mg exposed to an aqueous solution, is expected to be many orders of magnitude larger than that for steel exposed to an aqueous solution.

2.2. Alloying Influences

The corrosion mechanism implies two important alloying influences on the corrosion performance of Mg alloys: (1) the cathodic (*H* evolution) reaction on second phases and (2) surface films. The important influence of the cathodic reaction is a theme throughout the following. A surface film comparable to that on stainless steels might produce stainless Mg as suggested by Song and Atrens,[1,2] and Atrens,[20] and is the aim of current research. Prior work has not discovered any alloying addition that has led to a Mg alloy with a corrosion performance significantly better than that of pure Mg in a practical environment like an aqueous 3 % NaCl solution. Data does exist[3] that indicated that corrosion rates for Mg-Al alloys decreased with increasing Al content. However, that data[3] appears to have been for low purity alloys, and the decrease in corrosion rate appears to have been related to a decrease in the impurity level with increasing Al content. More recent data,[35] presented in Figure 3, compared the corrosion rates of high purity alloys (HP-Mg, HP-Mg1Al, HP-Mg5Al, MEZ, AM60 and AZ91D) with those of low purity Mg (CP-Mg) in the salt immersion test (3 % NaCl)(SIT) and the salt spray test (SST). This data showed that the high purity alloy with 1 %Al (HP-Mg1Al) had a corrosion rate comparable with that of high purity Mg (HP-Mg) and high purity commercial Mg alloys (MEZ, AM80 and AZ91D). Moreover, the high purity alloy containing 5 % Al (HP-Mg5Al) had a corrosion rate significantly higher than that of high purity Mg (HP-Mg) due to the micro-galvanic corrosion acceleration of the corrosion of the α phase by the adjacent β phase.

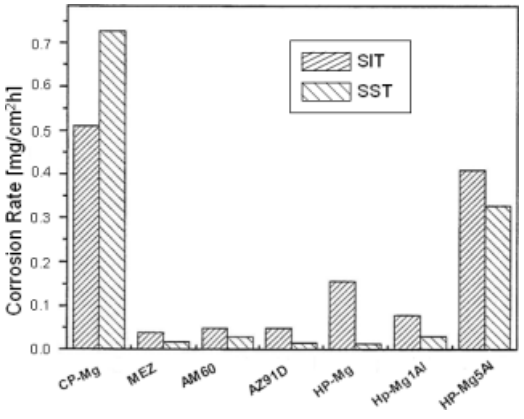

Fig. 3. Comparison of the corrosion rates of high purity alloys (HP-Mg, HP-Mg1Al, HP-Mg5Al, MEZ, AM80 and AZ91D) with those of low purity Mg (CP-Mg) in the salt immersion test (3 % NaCl SIT) and salt spray test (SST). [35]

The influence of minor contaminants (Fe, Ni, Cu, and Co) on the corrosion performance of Mg alloys can also be understood[1,2] in terms of the corrosion mechanism, and in particular that the cathodic partial reaction is *H* evolution, Equation 1. Hanawalt et al.[65] found that four elements (Fe, Ni, Cu, and Co) had a profound accelerating effect on the salt-water corrosion rate. Subsequent studies have confirmed that purity is a critical factor in the corrosion of Mg alloys. Corrosion rates were accelerated 10-100 fold when the concentration of the critical contaminants (Fe, Ni and Cu) was above a critical tolerance level.[66] Fe, Ni, Cu and Co have extremely deleterious effects because of their abilities to serve as active cathodic sites.[67] For each of these elements a "tolerance limit" can be defined. When the impurity content exceeds the "tolerance limit", the corrosion rate is high, whereas, when the impurity content is lower than the "tolerance limit", the corrosion rate is low.

2.3. Alloy Classes

The corrosion mechanism provides an understanding of why there are essentially two classes of Mg alloys in relation to corrosion performance.[2] These alloy classes are (1) Zr containing alloys and (2) Zr free alloys.

2.3.1. Zr Containing Alloys

Zr reacts with the impurity elements Fe, Ni, Co and Cu removing them from the melt thus producing intrinsically "high-purity" alloys with good corrosion properties comparable to the corrosion properties of pure Mg.[68,69] The removal of the impurity elements like Fe from the alloy by Zr is an incidental reaction and is not related to the direct reason that Zr is used as an alloying element, which is that Zr is an effective grain refiner. Zr also reacts with Al, so alloying with Al is incompatible with alloying with Zr. The Zr containing alloys often contain alloying additions like RE, Ag, Th etc, that allow the production of good mechanical properties. These alloys tend to be expensive and are largely restricted to applications where cost is less important than good properties, applications such as in the aerospace industry.

2.3.2. Zr free Alloys

The most common are the alloys containing Al, such as AZxx, AMxx and ASxx. Their corrosion resistance is highly dependent on the contents of the impurity elements Fe, Ni, Cu and Co. High purity versions show corrosion rates comparable with high purity Mg and the Zr containing alloys.

For these alloys, second phases have a pronounced influence on the corrosion rates. For example, an alloy with a high Al content like AZ91 has typically an appreciable amount of β, $Mg_{17}Al_{12}$, along the grain boundaries. $Mg_{17}Al_{12}$ is cathodic with respect to the matrix, as are most second phases in Mg-base alloys.[70] Furthermore, the β phase had a higher cathodic activity than the α phase.[24,25] Consequently, the β phase has two influences on corrosion, as a barrier and as a galvanic cathode, depending on the volume fraction and distribution of β in the α matrix. The β phase acts as a galvanic cathode and accelerates the corrosion of the α matrix if the volume fraction of β phase is small. However at high volume fractions, the β phase can act as an anodic barrier to inhibit the corrosion of the alloy, if the β phase forms an interconnected network.

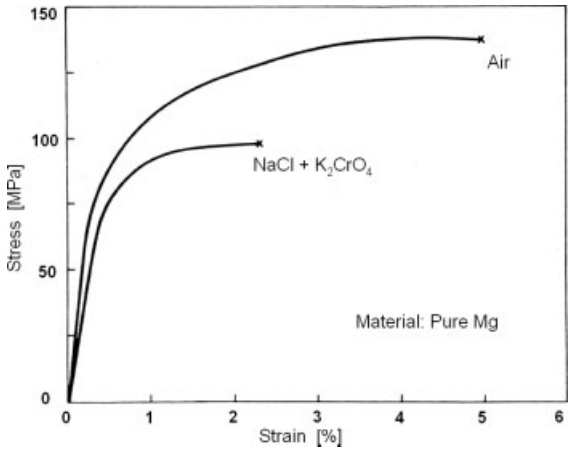

Fig. 4. Stress-strain curves for pure Mg in air and in 3.3 wt% NaCl + 2 wt% K_2CrO_4. [72]

2.4. Environment Influences

No material is corrosion resistant in all environments. High corrosion resistance always refers to some particular environment. A particular material could have a high corrosion resistance in a particular environment but a low corrosion resistance in another. The various environmental influences,[1–3,20] may be understood using the principles of the corrosion mechanism. Corrosion, in general, needs a liquid water phase, so the corrosion rate is low in dry air, dry gases, and in many organic solvents. Corrosion rates, in aqueous solutions, are low under conditions, which promote the formation of a stable corrosion product film. For example, (1) local conditions of pH above 10.5 (to produce a film of $Mg(OH)_2$), including stagnant pure water, (2) fluoride containing solutions (insoluble MgF_2 film), (3) $MgSO_4$ in concentrated sulphuric acid, and (4) oxidising conditions free of film breakdown agents like chlorides can lead to stable oxide/hydroxide films. Surface films can lead to low corrosion rates. Fracture of such films by an applied stress may be part of an SCC mechanism. In contrast, high corrosion rates are experienced under conditions leading to surface-film beak down (e.g. chloride solutions). Corrosion rates are also high for Mg in galvanic contact with heavy metals, or for Mg with surface contaminated with a heavy metal (e.g. a magnesium surface shot blasted with Fe shot (see Sec. 7)), or Mg in contact with a solution of heavy metal salts.

3. Phenomenology of SCC

3.1. Alloy Influences

3.1.1. Pure Mg

Pure Mg is susceptible to SCC.[71–73,75] Meletis and Hochman[72] reported that TGSCC was crystallographic for 99.9 % pure Mg subject to an applied strain rate of 1.7×10^{-5} s^{-1} in a chloride-chromate solution. Figure 4 shows that the failure in the solution occurred at 68 % of the fracture strength in air and that the strain to failure in the solution, ε_{sol}, was 55 % of the strain to failure in air, ε_f. Fracture surfaces were interpreted as being due to cleavage-like fracture, consisting of flat, parallel facets on {2203} planes separated by steps also on {2203} planes. Based on the fracture surface topography, the observation that SCC was accompanied by *H* evolution and that cracking was initiated at corrosion pits, the authors speculated that cleavage was induced by a reduction in the surface energy of the cleavage plane, due to atomic *H* accumulation or the formation of Mg hydride.

Stampella et al.[75] reported that commercial purity Mg (99.5 %Mg) and high purity Mg (99.95 %Mg) failed by ductile tearing in laboratory air. SCC occurred in deaerated, pH=10, 10^{-3}M Na_2SO_4 solution. Failures for commercial purity and high purity Mg occurred at 79 % and 73 % of their ultimate tensile strengths, respectively, and the strain to failure in the solution, ε_{sol}, was 65 % and 55 % of the strain to failure in air, ε_f, respectively. They proposed that cracking occurred by HE induced cleavage initiated at corrosion pits. This proposal was based on the following observations:

– The mechanical response was similar for specimens tested in the solutions and for pre-exposed specimens (see Fig. 5) and SCC occurred at slow strain rates.

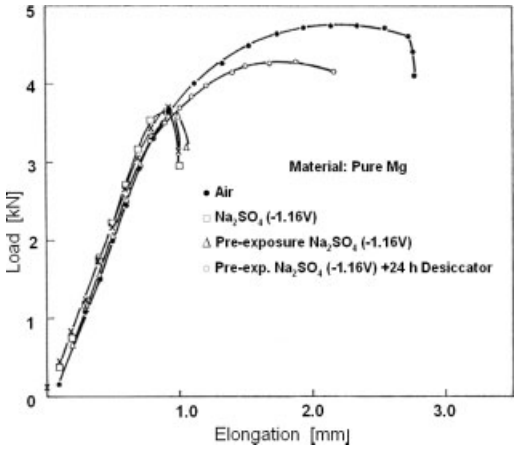

Fig. 5. Load versus elongation at a strain rate of 5.7×10^{-6} s^{-1} for commercial purity Mg anodically polarised to –1.16 V. ● Stressed in air; □, × stressed in Na_2SO_4 solution; △ pre-exposed to Na_2SO_4 solution and stressed in air; ○ pre-exposed to Na_2SO_4 solution, stored for 24 h and stressed in air. [75]

– The environment effect for pre-exposed specimens was partly reversible by storing for 24 h in a desiccator.
– SCC was invariably accompanied by pitting.
– SCC was prevented by cathodic polarisation (which inhibited pitting).
– SCC specimens exhibited cleavage-like fracture surfaces.

That the environment effects in pre-exposed samples were reversible was thought to preclude the involvement of stable Mg hydride precipitates or high-pressure *H* bubbles in the cracking mechanism. Instead, Stampella et al proposed that atomic *H* in solid solution facilitated cleavage. Stampella et al also proposed that the crack morphology was determined by the grain size (see Sec. 3.1), and that for fine grained (0.025 mm) commercially pure Mg, SCC was exclusively transgranular (TG) whereas for larger grained (0.075 mm) HP Mg, SCC was mixed, TG and intergranular (IG).

Lynch and Trevena[71] studied SCC of cast 99.99 % pure Mg in an aqueous 3.3 wt%NaCl + 2 wt%K_2CrO_4 solution, by cantilever bending of specimens at various deflection rates. They proposed that SCC occurred by localised microvoid coalescence resulting from dislocations at crack tips, due to weakening of interatomic bonds by adsorbed *H* atoms. They observed concave features on opposing fracture surfaces, so that the opposing fracture surfaces were not matching (see Sec. 4.2). They suggested that tubular voids were nucleated at intersections of {0001} and {101X} slip bands resulting in a fluted fracture surface parallel to {101X} planes as illustrated in Figure 6. It was reported that fractographic evidence of SCC was apparent for crack velocities between 10^{-8} and 5×10^{-2} m/s. They proposed that, thoughout this velocity range, SCC was induced by adsorption of *H* since insufficient time was available for *H* diffusion or localised dissolution at the crack tip. At the lower bound of this velocity range, it was conceded that there might be some *H* diffusion ahead of the crack tip. No fractographic evidence of Mg hydride formation was apparent for any velocities in this range (see Sec. 4.2.2).

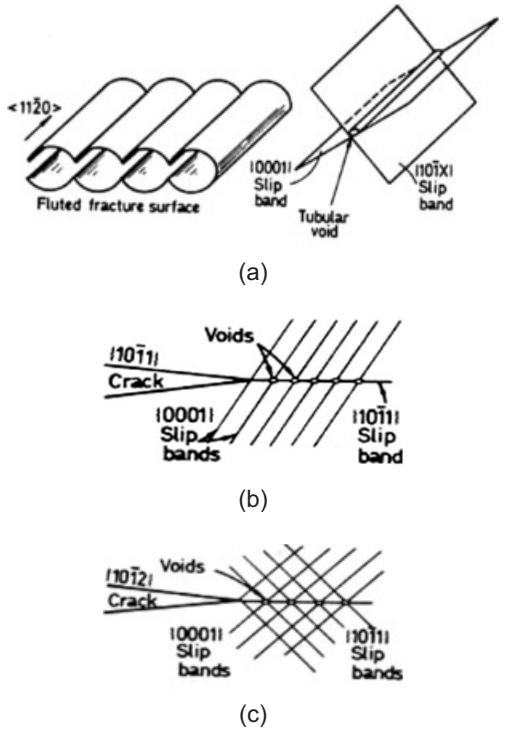

Fig. 6. Formation of fluted fracture topography by localised microvoid coalescence. [71]

3.1.2 Alloy Composition

The chemical composition of some common Mg alloys is given in Table 1. The common designation for Mg alloys can be illustrated by AZ61. In this designation, the first two letters

Table 1. Chemical composition (wt% unless ppm) of common Mg alloys [74–78].

	CP Mg[75]	HP Mg[75]	MA1[74]	MA2[74]	MA5[74]	AZ61[76]	AZ80[76]	AZ91[77]	ZE41[78]	ZK51[78]
Al	0.015	0.004		3–4	7.8–9.2	6.4	8.2	8.5–9.5		
Zn	0.003	0.003		0.2–0.8	0.2–0.8	0.95	0.8	0.45–0.9	3.5-5	3.5–5.5
Mn	0.01	0.004	1.3–2.5	0.15–0.5	0.15–0.5	0.17	0.2	0.17–0.4	<0.15	
Si	0.02	0.006						0.05		
Fe	0.02	0.003				0.004	0.005	0.004		
Cu	0.001	0.001						0.025	<0.1	<0.1
Ni	0.002	0.002						0.001	<0.01	<0.01
Be								5–15ppm		
Sn	0.005	0.005								
Ca	0.001	0.001								
Pb	0.005	0.005								
Cd	0.0001	0.0001								
Nd									0.75–1.75	
Zr									0.4–1	0.5–1

Table 2. SCC tendency of common alloys.

Alloy	Metallurgical Condition, Testing Details, Environment	SCC Threshold, σ_{SCC} or K_{1SCC}, Velocity, V	Ref
99.9% pure Mg	Heat treated to produce coarse grains, 5 h at 550 °C FC, Slow strain rate, 1.7×10^{-5} s^{-1}, 3.3% NaCl + 2%K_2CrO_4	TG crack plane {20$\bar{2}$3} direction [1$\bar{1}$01] authors deduced crystallographic fracture although fractography provides evidence of some ductility, UTS_{sol} = 68% UTS_{air}, V = 4–16 × 10^{-6} m/s	[72]
99.5% pure Mg	Annealed (20 μm grain size), Slow strain rate tests, plain specimens at 6×10^{-6} s^{-1}, 10^{-3} M Na_2SO_4, anodically polarised	TG quasicleavage, SCC initiated at surface pits. (Unstressed material undergoes severe pitting with a network of fine cracks around each pit.)	[75]
99.95% pure Mg	Annealed (75 μm grain size), Slow strain rate tests, plain specimens at 6×10^{-6} s^{-1}, 10^{-3} M Na_2SO_4, anodically polarised	IG & TG	[75]
99.99% pure Mg	As-cast, large grain size > 3 mm. Fatigue pre-crack in cantilever, loaded for range of deflection rates, 3.3% NaCl + 2% K_2CrO_4	IG & TG. Opposing surfaces were not interlocking, both had concave features, shallow flutes on {10$\bar{1}$X} planes, with cleavage like cracks/secondary facets also on same planes. V = 10^{-8} to 50 × 10^{-3} m/s, inceased with speed of loading	[71]
HP Mg	Annealed sheet, spring loaded, partial immersion in 0.5%KHF, YS = 5.0 tons/in^2	TG, σ_{SCC} = 3 tons/in^2 = 60%YS	[90]
Mg2%Mn	Annealed sheet, spring loaded, partial immersion in 0.5%KHF, YS = 8.6 tons/in^2	TG, σ_{SCC} = 4 tons/in^2 = 50%YS	[90]
MgMnCe	Mg1.5%Mn0.15–.5% Ce0.15% Al0.015% Fe, YS = 150 MPa, UTS = 240 MPa, e_f = 20%, constant stress in air, 0.001N NaCl, 0.01N NaCl, 0.01N Na_2SO_4	TG, σ_{SCC} = 85%YS	[97]
Mg2Mn.5Ce Mg3Al, AZ31, ZK31	Commercial alloys, annealed sheet, constant deflection test (plastic deformation) in distilled water and 0.5% KHF	TGSCC	[90]
ZK60A-T5	Extrusion, long term exposure to rural atmosphere	σ_{SCC} = 100MPa ~ 50% YS	[100]
ZE10	Extrusion, long term exposure to rural atmosphere	σ_{SCC} ~ 50% YS	[100]
ZK60A-T5	Artificially aged (T5), Distilled water	IG & TG, K_{1SCC} = 6 MPa$\sqrt{m}$, V = 1 × 10^{-8} m/s	[105]
ZK60A-T5	Artificially aged (T5), 1.4m Na_2SO_4	IG & TG, K_{1SCC} = 8 MPa$\sqrt{m}$, V = 4 × 10^{-6} m/s	[105]
ZK60A-T5	Artificially aged (T5), 5m NaBr	IG & TG, K_{1SCC} = 12 MPa$\sqrt{m}$, V = 10 × 10^{-6} m/s	[105]
QE22	Long term exposure to rural atmosphere	σ_{SCC} ~ 70–80% YS	[100]
HK31	Long term exposure to rural atmosphere	σ_{SCC} ~ 70–80% YS	[100]
HM21	Long term exposure to rural atmosphere	σ_{SCC} ~ 70–80% YS	[100]
AM60	"high purity" commercial alloy, as die cast, dead weight tension tests in distilled water, long term tests up to 500 day	σ_{SCC} ~ 40–50% YS	[84]
AS41	"high purity" commercial alloy, as die cast, dead weight tension tests in distilled water, long term tests up to 500 day	σ_{SCC} ~ 40–50% YS	[84]
Mg-1%Al	1h at 400 °C WQ, single α phase, Dead loaded wires, 40 g/L NaCl + 5–40 g/L K_2CrO_4	TG, σ_{SCC} = 85 MPa	[76]
Mg-3%Al	1h at 400 °C WQ, single α phase, Dead loaded wires, 40 g/L NaCl + 5–40 g/L K_2CrO_4	TG, σ_{SCC} = 83 MPa	[76]
Mg-6%Al	1h at 400 °C WQ, single α phase, Dead loaded wires, 40 g/L NaCl + 5–40 g/L K_2CrO_4	TG, σ_{SCC} = 77 MPa	[76]
AZ61	1h at 400 °C WQ, single α phase, Dead loaded wires, 40 g/L NaCl + 5–40 g/L K_2CrO_4	TG, σ_{SCC} = 77 MPa	[76]
AZ80	1h at 400 °C WQ, single α phase, Dead loaded wires, 40 g/L NaCl + 5-40 g/L K_2CrO_4	TG, σ_{SCC} = 65 MPa	[76]
LP AZ31B	Extruded, CERT, 2–8% NaCl, distilled water	TG quasicleavage	[91]
AZ31B	Annealed, Dead load, 40 g/L NaCl + 5–4 0g/L K_2CrO_4	σ_{SCC} = 96%YS	[115]
AZ31	Annealed at 150 °C, UTS = 240 MPa, Dead load, 40 g/L NaCl + 5–40 g/L K_2CrO_4	σ_{SCC} = 235 MPa ~ 98%UTS	[15]
AZ31	Annealed at 150 °C, UTS = 240 MPa, Spring and dead load, Coastal atmosphere	σ_{SCC} = 140 MPa ~ 60%UTS	[15]
AZ31	Annealed at 150 °C, UTS = 240 MPa, Spring and dead load, Rural atmosphere	σ_{SCC} = 100 MPa ~ 40%UTS	[15]
AZ31	YS = 150–180 MPa, Atmosphere	σ_{SCC} = 60%YS	[15]
AZ61	Annealed at 190 °C, UTS = 230 MPa. Dead load, 40g/L NaCl + 5–40 g/L K_2CrO_4	σ_{SCC} = 210 MPa ~ 90%UTS	[15]

Table 2. Continued.

AZ61	Annealed at 190 °C, UTS = 230 MPa, Spring and dead load, Coastal atmosphere	σ_{SCC} = 120 MPa ~ 50%UTS	[15]
AZ61	Annealed at 190 °C, UTS = 230 MPa, Spring and dead load, Rural atmosphere	σ_{SCC} = 100 MPa ~ 40%UTS	[15]
AZ61	Annealed at 330 °C, UTS = 170 MPa, Direct load, 40g/L NaCl + 5–40 g/L K_2CrO_4	σ_{SCC} = 140 MPa ~ 80%UTS	[15]
AZ61	Annealed at 330 °C, UTS = 170 MPa, Spring load, Coastal atmosphere	σ_{SCC} = 100 MPa ~ 60%UTS	[15]
AZ61	Sheet material, atmospheric conditions	σ_{SCC} ~ 55%YS	[74] [i]
HP AZ61	Extruded, ST 24h at 345 °C FC, Three-point bending under constant deflection, initial stress above yield, 3% NaCl + 3% K_2CrO_4	IG	[80]
HP AZ61	Extruded, ST 24h at 345 °C WQ, Three-point bending under constant deflection, initial stress above yield, 3% NaCl + 3% K_2CrO_4	TG along {0001}	[80]
HP AZ61	CW, 90 s at 400 °C, 1 h at 200 °C, fine grained 5 μm, heavy $Mg_{17}Al_{12}$ GB precipitate, Dead loaded wires, 40 g/L NaCl + 5–40 g/L K_2CrO_4	IG, σ_{SCC} = 85 MPa	[94]
HP AZ80	CW, 90 s at 400 °C, 1 h at 200 °C, fine grained 5 μm, heavy $Mg_{17}Al_{12}$ GB precipitate, Dead loaded wires, 40 g/L NaCl + 5–40 g/L K_2CrO_4	IG, σ_{SCC} = 100 MPa	[94]
HP AZ61	Extruded, strain annealed, ST 24 h at 480 °C WQ, Three-point bending under constant deflection, 40 g/L NaCl + 40 g/L K_2CrO_4	TG, discontinuous	[95]
HP AZ61	Extruded, ST 24 h at 345 °C FC, Three-point bending under constant deflection, 40 g/L NaCl + 40 g/LK_2CrO_4	IG, continuous	[95]
HP AZ61	As-rolled, Single edge notched (FM) specimens, 3.5% NaCl + 2% K_2CrO_4	IG, K_{1SCC} = 14 – 17 MPa$\sqrt{m}$	[93]
HP AZ61	Rolled, 1.5 h at 475 °C, quenched, aged 48 h at 200 °C, Single edge notched (FM) specimens, 3.5% NaCl + 2% K_2CrO_4	IG & TG, K_{1SCC} = 12–13 MPa$\sqrt{m}$	[93]
AZ61	6.5% Al, 1.1% Zn, 0.02% Fe, cold drawn, annealed at 350 °C WQ, direct loaded wire exposed to 4% NaCl + 4% K_2CrO_4 pH = 8	TG, σ_{SCC} = 100 MPa, discontinuous propagation	[92]
AZ61	6.5%Al, 1.1%Zn, 0.02%Fe, cold drawn, annealed at 350 °C WQ, direct loaded wire exposed to 4% NaCl + 4% $K_2Cr_2O_7$ pH = 5	TG, σ_{SCC} = 70 MPa, discontinuous propagation	[92]
AZ61-F	Extrusion, long term exposure to rural atmosphere	σ_{SCC} = 30% YS	[100]
AZ63-T6	Sand cast, long term exposure to rural atmosphere	σ_{SCC} = 60% YS	[100]
HP Mg-7Al	Extruded, ST 1hr at 350 °C, 7 various aging treatments, Constant stain and slow strain rate tests at 5×10^{-2} to 10^{-6} s^{-1}, Dead weight loaded pre-cracked cantilever specimens, 35 g/L NaCl + 20 g/L K_2CrO_4	TG (except for IG for one HT), σ_{SCC} ~ 0.1% proof stress. K_{1SCC} linearly related to σ_{th} by eq(9), V = 2–5 × 10^{-6} m/s for plain and pre-cracked specimens	[85]
Mg-7.6Al	Rolled, ST 4 h at 385 °C WQ, single α phase, 70 μm grain size. Constant deflection tensile loading of notched sheet specimens, 40 g/L NaCl + 40 g/L K_2CrO_4	TG, V = 6 to 42 × 10^{-6} m/s	[121]
HP Mg-7.61Al	Hot rolled, coarse grains ~ 12 mm, ST 4 h at 385 °C WQ, single α phase, Three-point bending under constant deflection of a single grain, 4% NaCl + 4% K_2CrO_4	TG, Interlocking opposing surfaces {31$\bar{4}$0} planes, Intermittent crack advance ~ 0.1 μm at 250 s^{-1}, V = 18 × 10^{-6} m/s	[86]
HP Mg-8.6Al	Extruded, ST 70 h at 420 °C WQ, Constant deflection in tension, distilled water	TG, opposite faces had matched faceted topography, SCC at 66% of notched UTS	[87]
HP Mg-8.6Al	Extruded, ST 70 h at 420 °C WQ, Constant deflection in tension, 3.5% NaCl + 2% K_2CrO_4	TG, opposite faces had matched faceted topography, SCC at 50% of notched UTS	[87]
HP AZ91E	Sand cast, T6, DCB, 3.5% NaCl	K_{1SCC} = 7.5MPa$\sqrt{m}$	[101]
AZ91	"high purity" commercial alloy, as die cast, dead weight tension tests in distilled water, long term tests up to 500 day	σ_{SCC} ~ 40–50% YS	[84]
AZ91	"low purity" commercial alloy, as die cast, dead weight tension tests in distilled water, long term tests up to 500 day	σ_{SCC} ~ 40–50% YS	[84]
Mg-1Al, Mg9Al	As-cast or rapidly solidified, Constant displacement rate tests with pre-cracked ribbons, 0.6M NaCl + 0.2M K_2CrO_4	TG, V = 0.1 to 10 × 10^{-6} m/s, depending on displacement rate	[83]
Mg-9Al	Extruded, ST 4 h at 350 °C WQ, single α phase, 20 μm grain size. Slow strain rate tests of plain specimens at 3 × 10^{-5} s^{-1} and constant load and constant deflection tests of pre-cracked specimens, 20 g/L NaCl + 5–20 g/L K_2CrO_4	TG, σ_{SCC} ~ 100 to 140 MPa, 40–50% of 0.2% proof stress, depending on solution. K_{1SCC} = 7–14 MPa$\sqrt{m}$, 20 – 40% of K_{1C}; linear relation between σ_{th} and K_{1SCC}. V = 0.1 to 5 × 10^{-6} m/s, depending on solution.	[107]

refer to the main alloying elements as follows: A aluminium, C copper, E rare earths, J Strontium, K zirconium, M manganese, Q silver, S silicon, X calcium, Z zinc, etc. The concentration of the alloying elements is given by the two numbers. Thus AZ61 nominally contains 6 %Al and 1 %Zn. In the literature, there are alloy designations that do not follow this convention, such as MA1, MA2 (AZ31) and MA5 (AZ91).

Table 2 provides an overview of the SCC tendencies of a range of common alloys and Table 3 provides information for alloy + environment combinations for which there are reports of SCC resistance.

Influence of Al: All Mg alloys have been reported to be susceptible to SCC to some extent.[79] Alloys containing Al are thought to be particularly susceptible in air, distilled water and chloride-containing solutions.[80] In such alloys, SCC-induced fractures may occur at stresses as low as 50 % of the yield strength. Various reports state that the threshold for SCC susceptibility occurs at 0.15–2.5 % Al.[9,73,75] Susceptibility is reported to increase with Al content with maximum susceptibility occurring at 6 % Al.[81] Other reports state that susceptibility does not vary for Al contents between 4 % and 9%.[73] Figure 7 shows that susceptibility (characterized in this case by time to failure as a function of initially applied stress and/or the threshold stress for SCC) increased as the Al content increased from 1 % to 8 %.

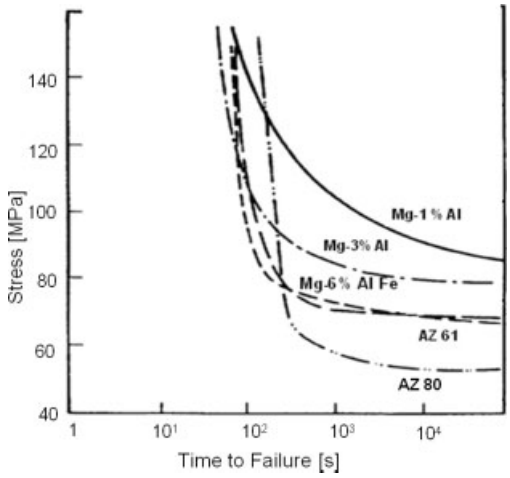

Fig. 7. Initial applied stress vs time to failure for various Mg-Al and Mg-Al-Fe alloys in chloride-chromate solutions. [76]

Al is used as an alloying element in Mg alloys to increase strength. Makar et al.[83] showed that increasing the Al content from 1 to 9 % dramatically increased the repassivation rate of Mg alloys, attributed to the superior passivation characteristics of Al. This might be expected to retard SCC as bare metal surfaces resulting from surface film rupture are required for preferential corrosion of the exposed substrate,

Table 3. Alloy + environment combinations for which there is information regarding SCC resistance, but consult Table 4 for threshold values.

Alloy	Metallurgical Condition, Environment	SCC Resistance	Ref
Mg2%Mn	Industrial atmosphere	"for practical purposes not susceptible to SCC"	[74]
Mg2% Mn0.24%Ce	Industrial atmosphere	"for practical purposes not susceptible to SCC"	[74]
Mg alloys with Al > 1.5%		Magnesium alloys containing more than 1.5% Al are susceptible to SCC. Wrought alloys appear more susceptible than cast alloys. While there is little documentation of service SCC of castings, laboratory tests can cause SCC at tensile loads less than 50% of yield stress in environments causing negligible corrosion. The low incidence of service SCC failures can be attributable to low actual stresses in service in the past.	[9]
AZ31	Industrial atmosphere	"very slightly susceptible to SCC"	[74]
AZ61, AZ91	Industrial atmosphere	"highly susceptible to SCC"	[74]
AZ61	Humid atmosphere	No SCC if RH < 95%	[74]
AZ61 sandwiched between sheets of Mg2%Mn	Marine atmosphere	No SCC for an applied stress less than 210 MPa	[74]
AZ81 sandwiched between sheets of Mg2%Mn	Atmosphere	No SCC in 200 d for an applied stress less than 150 MPa, whilst unprotected sheets cracked in a few days	[74]
AZ61	Mg alloy in service in atmospheric exposure	All service SCC examined by Dow Chemical Co has been attributed to residual stresses	[15]
AZ31, AZ61	Aircraft wing skins in Naval aircraft	"good service experience", few SCC cases, service SCC attributed to residual stress	[15]

which is an essential step in the TGSCC mechanism (see Sec. 4). They also reported that the Al extended the pH range over which Mg alloys form a protective film. By analyzing the passivating $Mg(OH)_2$ surface film formed in water and aqueous environments using X-ray and electron diffraction techniques, Fairman and Bray[76] proposed that two Al^{3+} ions are incorporated into the tetrahedral $Mg(OH)_2$ lattice by replacing three Mg^{2+} ions resulting in vacant lattice sites. The resulting film is thicker and was considered to be more protective. This was used to explain the perceived increased general corrosion resistance of Mg-Al systems. However, the proposed influence of this film seems to have no dominating effect in 3 % NaCl solution as can be seen from Figure 3.

Relatively recent work by Miller[84] clearly showed that the most popular alloys, AZ91, AM60 and AS41, evinced SCC in distilled water. The specimens were partially immersed and it is important to note that SCC occurred at or close to the water-air interface. The time to failure data, for experiments lasting up to 500 days, can be interpreted to show a SCC threshold at ~40–50 % of yield strength for all three alloys. Miller tested both high purity versions of these commercial alloys as well as AZ91 containing a high iron content (0.01 %). The high iron alloy showed the same SCC behaviour as the high purity alloys, although the high iron AZ91 had poor corrosion resistance in salt spray testing.

Influence of Zn: The addition of Zn has also been reported to increase SCC susceptibility[16] although this was disputed by Fairman and Bray.[76] Mg-Zn alloys containing rare earths, such as the ZExx series of alloys, generally are considered to have moderate SCC susceptibility relative to Mg-Al-Zn alloys. The AZxx class of alloys contain both Al and Zn and are considered particularly susceptible in air and chloride-containing solutions. They are also the most commonly used, which is one reason why many studies of SCC in Mg alloys have focused on Mg-Al alloys,[85–90] on Mg-Al-Zn alloys[91–95] and on pure Mg.[71,72,75]

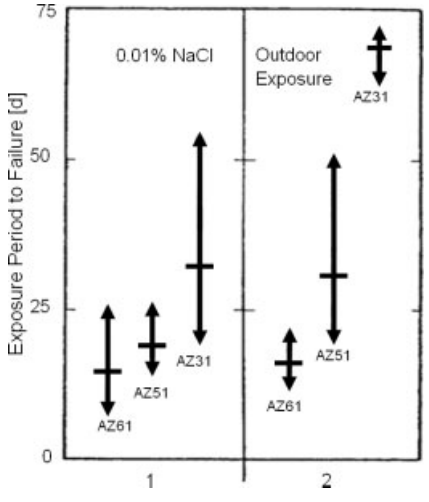

Fig. 8. Time to failure for (A) AZ61, (B) AZ51 and (C) AZ31 in (1) 0.01 % NaCl and (2) an outdoor environment. [82]

As discussed in Section 1.2, SCC occurs for specific combinations of alloy and environment.[11,96] A consequence is that a particular alloy can have different SCC lifetimes in different environments, as is illustrated in Figure 8, which shows that the three alloys have different lifetimes in the NaCl solution and outdoor environments. As a consequence, accurate prediction of SCC performance requires a detailed mechanistic understanding of the metal-environment interactions, backed by experimental evaluation of probable environments. The number of influential parameters is too large to allow a purely empirical approach.

Influence of Mn: Mg-Mn alloys have been generally considered to be immune in the atmosphere, chloride solutions and chloride-chromate solutions,[16] but have been reported to be susceptible in the atmosphere and in distilled water.[97] This tends to conflict with the commonly-proposed role of pitting in the initiation of stress corrosion. Chloride solutions generally promote pitting whilst distilled water promotes more uniform corrosion. In contrast to the general belief regarding SCC resistance of Mg-Mn alloys, Tomashov et al.[97] showed SCC for Mg-Mn alloys in solutions containing chloride and sulfate ions, and Perryman[90] showed SCC for commercial Mn-2 %Mn-0.5 %Ce in distilled water and 0.5 % potassium hydrogen fluoride solution. Timonova[74] stated that the addition of Mn or Zn to Mg-8 %Al decreased susceptibility; however, the addition of both elements together was stated to increase susceptibility.

Influence of Fe: Fe is present only as an impurity in Mg alloys and is reported to exist in Al-containing alloys in the form of various intermetallic compounds, each of which has a highly cathodic electrochemical potential relative to the primary phase. Fe tends to reduce corrosion resistance by promoting microgalvanic corrosion.[1–3,73] If *H* evolution is required for SCC, then it may be inferred that low-purity alloys might be more susceptible due to the higher availability of *H*. That FeAl contributes to SCC has been proposed by several authors.[80,90,98] Priest et al.[80] proposed that FeAl segregation occurs on the basal plane, and that cracking occurs on this plane by preferential corrosion of the bulk material adjacent to the FeAl. However, no conclusive evidence of basal segregation of FeAl has been provided. Fairman and Bray[76] stated that, although Fe contributes to general corrosion, it has minimal effect on SCC. Perryman[90] showed that, for Mg-5Al with 0.013 % and 0.0019 % Fe content (all other compositions being equal), the alloy with the higher Fe content was more susceptible in distilled water. In contrast, Miller[84] found equivalent performance in distilled water for low purity (0.010 %Fe) and high purity AZ91. Timonova[74] reported that Fe had no effect on the SCC of Mg-Al-Zn-Mn alloys. It has also been found that the concentration of FeAl is reduced by the presence of $Mg_{17}Al_{12}$ in which it is soluble.[90] Pelensky and Gallaccio[81] reported that SCC susceptibility for Mg-5Al alloys increased with Fe concentration. Pardue et al.[95] reported that the percentage of TG cracking in heat-treated AZ61 increased with Fe concentration.

Other elements: Reports are varied on the effects of other elements. Some sources suggested that the elements Li, Ag, Nd, Zr, Pb, Cu, Ni, Sn and Th had little or no influence on SCC susceptibility.[16,73] Conversely, Rokhlin[99] reported that the addition of Cd and Nd to a Mg-Zn-Zr alloy increased resistance to SCC. The ASM Handbook[73] stated that alloys containing Zr and other rare-earths can have intermediate susceptibility in atmospheric environments; however, Busk[79] stated that cast Mg-Zr alloys suffer from negligible SCC. It has also been reported that Cd, Ce and Sn may increase susceptibility in certain alloys.[73] This was supported by Timonova[74] who stated that small additions of Ce or Sn to Mg-Al-Mn alloys increased susceptibility.

3.1.3. Wrought v Cast

The majority of the SCC literature has focused on extruded or rolled Mg. Studies of SCC in cast Mg alloys have been few, although those that do exist have reported trends in susceptibility with respect to microstructure, composition and strain rate similar to those for wrought alloys. From the available information, it appears that SCC susceptibility is affected by the various factors which are related to the processing (casting and mechanical working) and subsequent heat treatment, such as the presence and distribution of the β phase and grain size (see Sec. 3.1.4 and Sec. 3.1.5). SCC susceptibility is also influenced by factors, which may be more significant for wrought alloys, such as microstructural defects and residual stresses.

Figure 9 shows that, for a given applied normalized stress, sand-cast AZ63 was less susceptible to SCC exposed to a rural atmosphere than extruded or rolled AZ61. This trend may be due to the influence of residual stresses or microstructural defects resulting from the extrusion or rolling processes. Stephens et al.[101] reported that cast AZ91E-T6 alloy (a high-purity variant of the commonly used AZ91C sand-cast alloy) was highly susceptible to SCC in aqueous 3.5 % NaCl. Lynch and Trevena[71] reported that SCC occurs by HE in 99.99 % pure Mg specimens cut from as-cast blocks in the 3.3 % NaCl + 2 % K_2CrO_4 solution.

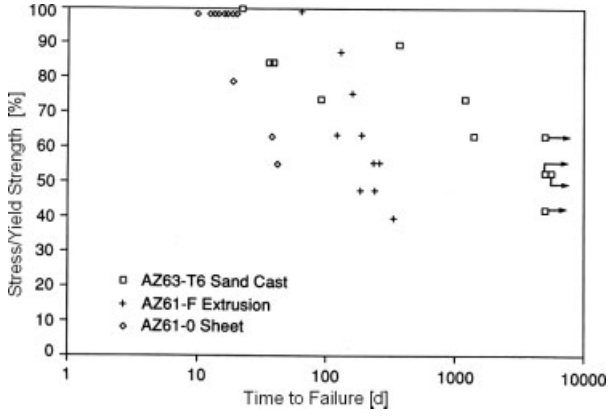

Fig. 9. Long term rural-atmosphere SCC susceptibility as characterized by normalized applied stress (as a percentage of yield strength) and time to failure for cast and wrought Mg alloys with similar composition. [100]

The casting process itself also influences SCC susceptibility for Mg alloys. Makar et al.[83] compared TGSCC characteristics of high-purity rapidly solidified (RS) and as-cast (AC) Mg-1Al and Mg-9Al alloys in the chloride-chromate solution, pH 9.0, containing 3.5 wt%NaCl + 4.0 wt% K_2CrO_4. They found that although the overall current densities for RS and AC alloys were similar, repassivation occurred more quickly in the RS alloys whilst corrosion in AC alloys was more severe and localized. The greater localized corrosion resistance and higher repassivation rate of the RS alloys was attributed to compositional and microstructural homogenization. Rapid solidification increased the solubility of Al in the Mg matrix from around 2 % (for as-cast alloys) to between 5 and 9 %. Therefore AC alloys were more likely to contain $Mg_{17}Al_{12}$ grain-boundary precipitates. Similarly, Mathieu et al.[102] stated that the concentration of Al in the primary α matrix for AZ91D alloys is 1.8 % for die cast alloys and 3 % for semi-solid cast alloys. The uniformity and corrosion protection provided by surface films is dependent on the structure and composition of the substrate. AC alloys tended to form less uniform surface films and to suffer from more localized corrosion due to galvanic interactions with the second phase. Localised corrosion is generally accepted to be involved in the inception of SCC by providing film-free surfaces at which *H* ingress may occur.[107] Die-cast alloys were more susceptible to SCC than RS and semi-solid cast alloys.

It has been shown that SCC resistance is reduced by residual tensile stresses.[73] Timonova et al.[103] stated that Mg-Y-Zn alloys have reduced SCC resistance in NaCl solution following hot deformation, and that resistance can be partly recovered by subsequent annealing. They attributed this to the removal of residual tensile stresses resulting from partial precipitation of a second phase ($Mg_{24}Y_5$). Marichev and Shipilov[113] observed that the SCC resistance of hot rolled Mg-Y-Zn alloy was anisotropic. Chakrapani and Pugh[86,88] proposed that SCC for hot-rolled Mg-7.5Al alloy in 4 wt%NaCl + 4 wt% K_2CrO_4 occurred by cleavage on $\{31\bar{4}0\}$ planes. The cleavage planes were orientated perpendicular to the rolling plane, so, for specimens loaded in bending, the direction of crack propagation was defined by the orientation of the tensile face with respect to the rolling plane. Timonova et al.[103] stated that for Mg-Y-Zn alloys formed by hot deformation, all anisotropy was removed by annealing.

3.1.4. Transgranular (TG) v Intergranular (IG)

Many workers[16] have stated that most SCC occurs by TG crack propagation. Others[72,75,80,94] claim that IG cracking is dominant for certain conditions. It appears that different driving mechanisms apply for IGSCC and TGSCC, and that these mechanisms are defined by the microstructure and the environment. For instance, Pardue at al.[95] proposed that TG cracking is discontinuous and involves alternating mechanical and electrochemical processes whereas IG cracking is con-

tinuous and completely electrochemical. It also appears likely that the same SCC mechanism (i.e. HE) may produce both TG and IG fracture, depending particularly on the grain size.

Stampella et al.[75] observed TG cracking for fine grained (25 μm) 99.5 % commercial-purity Mg whereas mixed TG-IG cracking occurred for large grained (75 μm) 99.95 % high-purity Mg. The IG cracking was attributed to the large grains being subject to higher stresses across grain boundaries, due to more concentrated dislocation pile-ups. In contrast, Meletis and Hochman[72] reported that 99.9 % purity Mg, heat-treated and furnace cooled to produce coarse grains, failed in a TG fashion.

It may be important to note that Stampella et al used a dilute 10^{-3} Na_2SO_4 aqueous solution whilst Meletis and Hochman used a chloride-chromate solution, suggesting that crack morphology was influenced by the environment. Further evidence of this effect was given by Perryman[90] who showed that Mg-5Al failed in a TG fashion in saturated $MgCO_3$ solution, 0.5 % KF solution, 0.5 % KHF solution and 0.5 % HF solution, whilst IG cracking occurred in a 0.05 % potassium chromate solution. If HE is the mechanism tending to produce TG cracking, then the critical parameter characterizing the solution-material interaction might be the effective *H* activity produced by each solution; it might be expected that a higher *H* activity might be linked to a greater tendency to produce TG cracking, even for a pure Mg with a large grain size.

Priest et al.[80] and Fairman and Bray[94] suggested that, for Mg-Al-Zn and Mg-Al alloys, heat treating to produce fine grains (~5 μm) results in IGSCC; however, it is important to note that the heat treatment resulted in heavy $Mg_{17}Al_{12}$ precipitation at grain boundaries. Fairman and Bray[94] stated that Mg-Al alloys are more inclined to fail in an IG manner if the Al content is greater than 6 %. This was based on the proposal that IGSCC occurred by preferential corrosion of the metal matrix immediately adjacent to the $Mg_{17}Al_{12}$ precipitate at grain boundaries as shown in Figure 10. Miller[16] and Pardue et al.[95] attribute all IGSCC to this micro-galvanic mechanism, although Priest et al also noted that some limit of the grain size was required to induce IGSCC regardless of the presence of $Mg_{17}Al_{12}$. The maximum grain size for IGSCC was found to be around 28 μm. Priest et al. proposed that where both IGSCC and TGSCC are possible, due to the presence of $Mg_{17}Al_{12}$ and a source of *H*, increasing the grain size causes a transition to TGSCC because the crack may propagate along a more direct path (or alternatively HE might be easier with a large grain size). Large grain sizes were induced by strain- annealing by reducing the rod length by 6 % and then heating to 480 °C. A more detailed discussion of the IGSCC mechanism is given in Section 4.1.

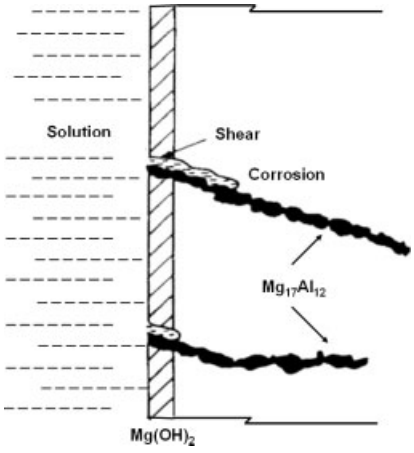

Fig. 10. Preferential corrosion of metal matrix adjacent to $Mg_{17}Al_{12}$. [94]

Mears et al.[104] showed that Mg-6.5Al-1Zn failed by IGSCC in the pH=5.0 chloride-bichromate solution (3.5 wt%NaCl + 2.0 wt%$K_2Cr_2O_7$) and by TGSCC in the pH=8.1 chloride-chromate solution (3.5 wt%NaCl + 4.0 wt%K_2CrO_4.). However, that crack morphology was influenced by pH was rejected on the basis of experimental evidence by Fairman and West[92] and Pardue et al.[95] It should be noted that Fairman and West tested single-phase Mg-7Al-1Zn in chloride-chromate solutions. According to the popular model for IGSCC (see Sec. 4.1) cracking in single-phase alloys is TG due to the absence of $Mg_{17}Al_{12}$. Also, Pardue et al tested large grained (~80 μm) Mg-6Al-1Zn in a chloride-chromate solution, which according to Priest et al.[80] would fail in a TG fashion due to the large grain size.

3.1.5. Heat Treatment

Detailed analyses of the influence of heat treatment on SCC susceptibility of Mg alloys are few. Speidel et al.[105] stated that the threshold stress intensity factor and stage 2 crack velocity for all high-strength magnesium alloys (including ZKxx) do not vary significantly with heat treatment. (Please see Sec. 3.2 for a description of the threshold stress intensity factor and stage 2 crack velocity). This would imply that SCC of high-strength Mg alloys does not depend on aging and also does not depend on slip morphology as is the case for high strength steels and high strength aluminium alloys.

However, the previous discussion on the roles of $Mg_{17}Al_{12}$ precipitates and grain size in determining crack morphology and in the IGSCC mechanism suggests that heat treatment does influence the SCC characteristics of Mg-Al alloys with grain sizes close to the IG-TG transition. $Mg_{17}Al_{12}$ may exist in Mg alloys with more than 2 % Al[83] and can be precipitated by slow cooling from the solution-treating temperature.[16]

Similarly, Priest et al.[80] showed that Mg-6Al-1Zn in chloride-chromate solutions failed in a TG fashion when heat treated for 24 h at 3456 °C and water quenched, and in an IG fashion when furnace cooled. $Mg_{17}Al_{12}$ was only precipitated in the furnace-cooled samples.

Moccari and Shastry[93] compared the SCC characteristics for rolled AZ61, as received and after two heat treatments. The two heat treatment consisted of annealing at 475 °C for 90 min, quenching in boiling water or iced brine, and aging at 200 °C for 48 h. The heat treatment did not significantly improve the SCC resistance. Quenching in iced brine resulted in a slightly higher threshold stress intensity factor relative to

quenching in boiling water; however, this trend was not significant enough for the authors to offer an explanation. It may be important to note that cracking for the as-received specimens was entirely IG whereas for the heat treated specimens some TGSCC was observed. This may suggest that, for the heat treated specimens, grain boundary precipitation was slightly discontinuous. It could be speculated that the difference in the threshold stress intensity factor for specimens quenched in boiling water and iced brine was due to differences in the $Mg_{17}Al_{12}$ concentration. Alternatively there could be a higher *H* activity facilitating (TG) *H* cracking.

Perryman[95] studied the influence of heat treatment on SCC susceptibility of Mg-5Al in distilled water. He found that the grain boundary precipitate was completely dissolved by solution treating at 360 °C for 3 h. Subsequent aging at 150 °C for 2 h to produce a continuous film of $Mg_{17}Al_{12}$ at grain boundaries had no significant effect on SCC behavior. It was inferred that, since cracking was TG, the precipitation of $Mg_{17}Al_{12}$ at grain boundaries was not significant. However, when precipitation was induced within grains by aging at 200 °C for 4 and 14 day, a reduction in localised pitting and an improvement in SCC resistance resulted.

Pardue et al.[95] investigated the effects of grain size and cooling rate on wrought AZ61 in a chloride-chromate solution. The specimens were heat treated at 345, 425 or 480 °C for 24 h and furnace cooled or quenched. The furnace cooled specimens had higher concentrations of $Mg_{17}Al_{12}$ precipitate at grain boundaries relative to the as-received specimens. Consequently, furnace cooled specimens failed primarily by IGSCC, whereas water quenched specimens had higher percentages of TGSCC. It was also observed that the specimens that were heat treated at 425 and 480 °C had larger grains than those treated at 345 °C. The percentage of TGSCC and the maximum corrosion current increased with increased grain size.

For specimens loaded in tension, residual tensile stresses are detrimental to SCC resistance whereas residual compressive stresses are beneficial to SCC resistance. The minimum applied stress required for SCC has been found to decrease with increasing residual tensile stress.[74] Busk[79] noted that residual tensile stresses reduced the threshold stress but could be adequately relieved by T4 (solution heat treated and aged to a stable condition) or T5 (artificially aged at an elevated temperature) heat treatments. If the T4 treatment involved quenching, then the resulting residual stresses could be adequately relieved by the heating phase of the T6 (solution heat treated and then artificially aged) treatment. Timonova[74] stated that relieving residual stresses in MA5 by annealing significantly increased SCC resistance with resistance increasing with annealing temperature.

Kiszko[106] stated that rapid cooling of Mg-14Li alloys with more than 1 % Al, after hot-working at 370 °C, increased susceptibility to SCC in humid air. SCC resistance was restored by heating at 150 °C for 24 h. The alloys failed in an IG fashion and it was proposed that SCC susceptibility of Mg-Li alloys was associated with the Al content and the formation of an unstable second phase during rapid cooling. This suggests that SCC occurs by corrosion adjacent to the Al-containing grain boundary precipitate. It should be noted that these Mg-Li alloys had a body-centered cubic crystal structure compared with that of most Mg alloys for which the α phase has the hexagonal close packed structure.

3.2. Loading

3.2.1 Fracture Mechanics Approach to SCC

There is no generalised analytical approach, based on micromechanics and physical metallurgy, which would allow prediction of which combinations of material and environment result in SCC. Consequently, the macro-mechanical approach of fracture mechanics is often used to gain insight into the phenomenon of SCC and to avoid or control SCC during service.

In general, damage-tolerant design practice accounts for initial flaws already existing in a structure or component, and fracture mechanics concepts are applied to characterise the conditions for initiation and growth of cracks from these flaws. Usually, stress corrosion cracks are considered to be macroscopically brittle, i.e. they occur at stresses below general yield and propagate in an essentially elastic body, even though local plasticity may be necessary for the cracking process. Therefore, linear elastic fracture mechanics (LEFM) is often used for studying SCC, and the crack tip stress intensity factor in the opening mode, K_I, represents the stress field in the vicinity of the crack tip and the mechanical driving force controlling the initiation of a crack and its further extension.

According to LEFM, the stress intensity factor at the crack tip is given by:

$$K_I = Y\,\sigma\,\sqrt{\pi a} \tag{8}$$

where *Y* is a geometric factor, σ is the applied stress and *a* is the crack length.

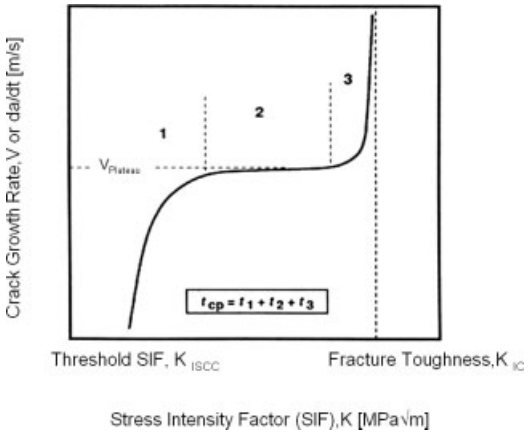

Fig. 11. Schematic of crack propagation velocity versus the stress intensity factor for a typical SCC system. [13]

In air, fracture occurs, when the value of K_I exceeds a critical value denoted by the fracture toughness of the material, K_{Ic}.

Experimental evidence has shown that, for a given material/environment combination, a unique relation exists between K_I and the growth rate of a stress corrosion crack. The usual way of representing this relationship is to plot the crack growth rate, da/dt (or v), as a function of K_I. In the typical schematic diagram, the so-called "v-K curve" (Fig. 11),[13] a value of K_I characterizes the level of the stress intensity factor at which the first measurable crack extension occurs, i.e. the threshold for SCC, K_{ISCC}. This, however, does not necessarily imply that there is, under all circumstances, a threshold in the sense of a real cut-off. On the contrary, for many material/environment combinations, the existence of a true threshold appears rather doubtful. The practical meaning of K_{ISCC} lies in the fact that below this stress intensity factor, the growth rates of stress corrosion cracks fall below a lower limit of e.g. 10^{-10} m/s, corresponding to a crack increment of roughly 3 mm per year.

The influence of the stress intensity factor, K_I, on the crack propagation velocity, involves three stages: initiation and Stage 1 propagation; steady-state or Stage 2; and final failure or Stage 3. It should be noted that Region 3 is not always observed; for example, Region 3 was absent in the work of Speidel et al.[105] for ZK60 in distilled water, 1.4 m Na_2SO_4 solution and 5 m NaBr solution (see Fig. 12). During Stage 1 propagation, the crack velocity increases rapidly as the stress intensity factor increases from K_{1SCC}. During Stage 2, the crack velocity is essentially constant. As the stress intensity factor approaches K_{1c}, the crack propagation mechanism becomes dominated by ductile tearing and rapid crack growth ensues until failure occurs. In Regions 1 and 3 crack velocity is strongly dependent on the stress intensity factor, whereas the steady-state crack velocity in Region 2 is largely independent of the stress intensity factor.[11–13,105] Quantitative prediction of crack velocities have to date not been particularly successful. Figure 13 shows that environmental conditions are among the parameters which influence steady-state crack velocity and the threshold values.[107]

It has been demonstrated that the results obtained from the different types of SCC tests, and on various specimen configurations, are identical if all specific requirements are carefully met. The data obtained from part through-cracked specimens can be used to predict crack initiation and growth in plates containing small semielliptical surface cracks, which simulate defects in large structures. This underlines the capability of the fracture mechanics approach to transfer SCC data

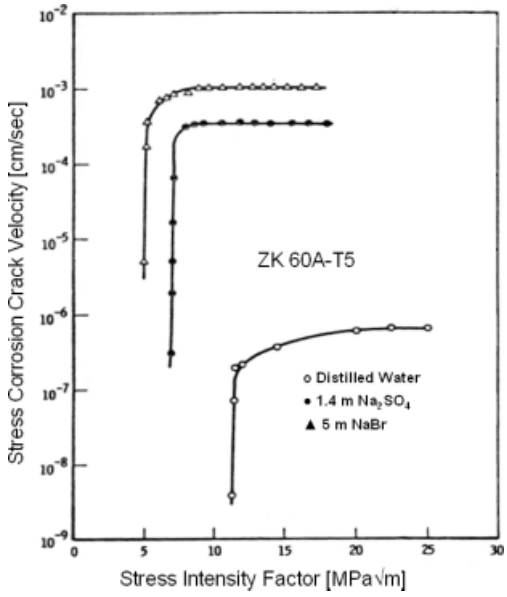

Fig. 12. Effect of the stress intensity factor on crack velocity for ZK60 alloy in various environments. [105]

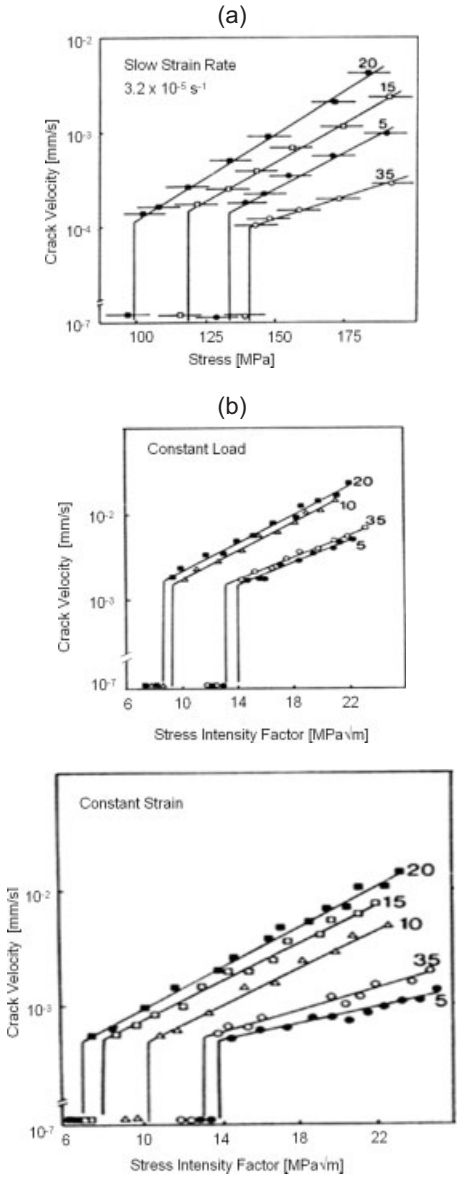

Fig. 13. Threshold stresses and stress intensity factors for Mg-9Al under various loading conditions in aqueous solutions with 35 g/L NaCl and various K_2CrO_4 concentrations (given in g/L). [107]

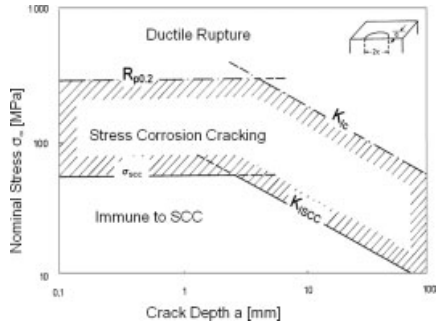

Fig. 14. Mechanical limits of a typical system involving an inert and a SCC environment. [11,12]

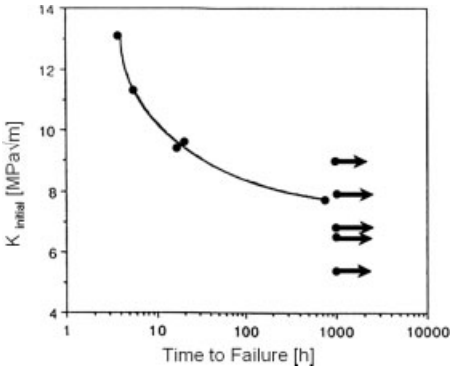

Fig. 15. Initial stress intensity factor versus time to failure for pre-cracked specimens. [101]

from small-scale laboratory specimens to real components and structures.

The advantage of using the parameter K_{ISCC} lies in its ability to predict the combinations of stress level, flaw size, and shape which leads to SCC. K_{ISCC} may be used as a design criterion for ensuring no SCC growth in service, provided that the stress levels, minimum detectable flaw sizes, and environmental conditions are well defined, and that the service loads are essentially sustained, i.e. that cyclic loading is not significant. Figure 14 schematically illustrates how K_{ISCC} values can be included in an assessment of structural integrity. In an inert environment, the mechanical limits are defined by the yield stress, σ_y, and the fracture toughness, K_{1C}. In an SCC environment, the mechanical limits are reduced to the threshold stress intensity factor, K_{1SCC}, and the threshold stress, σ_{SCC}, determined on smooth tensile specimens of the same material and in the same environment. These two parameters define an "acceptable region" with respect to immunity against SCC. Depending on the susceptibility of the material/environment combination under investigation, this region can be significantly smaller than the original "acceptable region" derived from tests in air.

For small cracks, the use of the K concept and hence of K_{ISCC} does become non-conservative, as is illustrated in Figure 14. Here, a combination of the SCC threshold stress, σ_{SCC}, determined on smooth specimens, and K_{ISCC} may serve as a "short crack" design criterion defining a minimum crack size for the use of the K concept.

3.2.2. Stress, Stress Intensity Factor and Strain Rate

The probability that SCC occurs increases with the sum of applied and internal tensile stresses.[11,74] It has been suggested that σ_{SCC} is related to the elastic limit or the yield strength of an alloy,[73,85] see also Table 2, however attempts to predict σ_{SCC} have not been successful. K_{1SCC} may be determined as illustrated in Figures 11 and 12, and may also be determined by plotting the initial stress intensity factor against the corresponding time to failure as illustrated in Figure 15. In this case, AZ91E-T6 specimens were fatigue pre-cracked in air to a crack depth of 0.45 to 0.55 of the specimen width before being stressed in 3.5 % NaCl solution.[101] The time to failure increased to large values as the initial applied stress intensity factor tended towards K_{1SCC}, which was around 7.5 MPa√m. Similarly, σ_{SCC} may be determined by plotting applied stress against the corresponding time to failure as illustrated in Figures 7 and 9.

Wearmouth et al.[85] examined the role of stress in the SCC of plain and pre-cracked Mg-7Al in a 3.5 wt% NaCl and 2 wt% K_2CrO_4 solution. They found that the SCC threshold stress, σ_{SCC}, was linearly related to the 0.1 % proof stress, $\sigma_{0.1PS}$. Moreover, they found that $\sigma_{SCC} \sim \sigma_{0.1PS}$ in contrast to subsequent research, particularly,[107] see also Table 2. They also reported that K_{1SCC} correlated with σ_{SCC} as illustrated in Figure 16. This relationship was defined by,

$$K_{ISCC} = c_1 + c_2\sigma_{SCC} \quad (9)$$

where c_1 and c_2 were constants. Ebtehaj et al.[107] who observed a similar relationship, suggested that this correlation was because, for pre-cracked or plain specimens, cracking was controlled by the strain rate, or alternatively cracks in plain specimens were initiated at corrosion pits such that they were essentially notched specimens. Both K_{1SCC} and σ_{SCC} represent the minimum values for which a crack would continue to

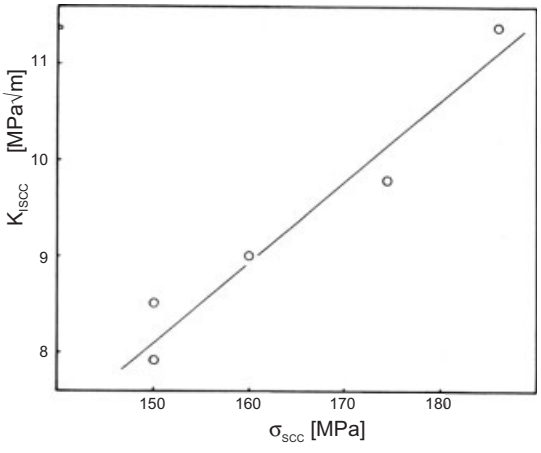

Fig. 16. Relationship between threshold stress and threshold stress intensity for Mg-7Al in a chloride-chromate solution. [85]

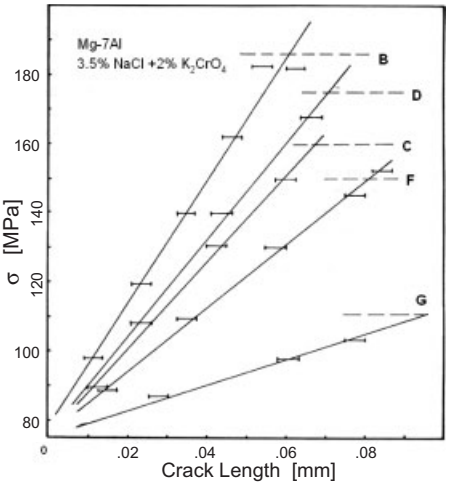

Fig. 17. Maximum non-propagating crack lengths for Mg-7Al in various metallurgical conditions. Corresponding threshold stresses are given as dashed lines. [85]

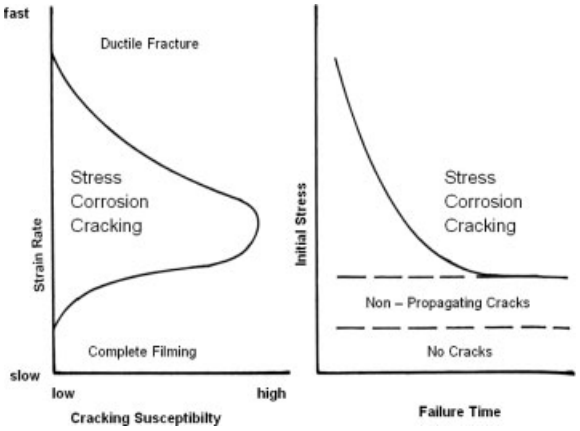

Fig. 18. Relationship between strain rate, initial stress and SCC susceptibility. [85]

propagate to total failure. However, Wearmouth et al also reported that plain specimens loaded below the threshold stress contained non-propagating cracks. Figure 17 shows that the maximum crack length for various material conditions (all promoting TG cracking) was proportional to the initial applied stress, and as the crack depth tended towards zero the applied stresses for all conditions converged on 75 MPa. For applied stresses below this value no cracking was detected. They also reported that the density of non-propagating cracks was proportional to the applied stress. Non-propagating cracks were also reported for heat treatments that induced IGSCC.

By combining Equations 8 and 9, Wearmouth et al determined that the non-propagating crack length corresponding to σ_{SCC} was given by

$$a_{cr} = c_3\left(\frac{K_{ISCC}}{\sigma_{SCC}}\right)^2 = c_3\left(\frac{c_1 + c_2\sigma_{SCC}}{\sigma_{SCC}}\right)^2 \qquad (10)$$

where c_3 was a constant. It was proposed that the threshold stress must be defined by principles of fracture mechanics.

Figure 18 proposed that the relationship between strain rate and SCC susceptibility was related to that between the initial applied stress and the time to failure. Stress levels greater than the threshold stress maintain strain rates such that repassivation is overcome and SCC may occur. For high stress levels, the strain rate is such that ductile fracture occurs faster than the SCC can progress. Below the threshold stress, the strain rates is insufficient to overcome repassivation.

Figure 13 shows that for Mg-9Al in chloride-chromate solutions, the threshold stress and the threshold stress intensity factor were environmentally dependent. Loose and Barbian[15] showed that SCC susceptibility was also dependent on the type of loading. Figure 19 shows time-to-fracture as a function of applied stress for cold rolled AZ61 (7.5, 15 and 22.5 percent total reduction) and annealed 1 h at 350 °C. The tests were conducted in a coastal outdoor environment, and the applied load was either axial or offset. The data illustrates how increasing the total reduction by cold rolling for the eccentrically-loaded specimens increased SCC resistance, whereas this had no significant effect on the axially-loaded specimens. This was attributed to the increasing creep rate and relaxation of stress with increasing amounts of cold work.

Constant load tests have been reported, in some particular circumstances, to be more severe than constant displacement tests[16,95] in that it has been found that SCC has occurred in constant load tests whereas the constant displacement tests have indicated no SCC susceptibility.[50] For constant load

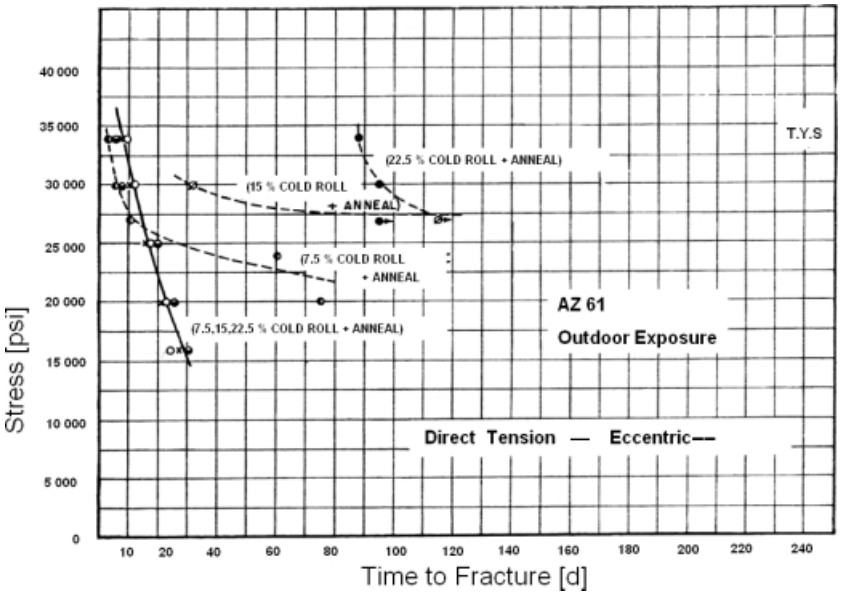

Fig. 19. Effect of axial and eccentric loading on SCC susceptibility of AZ61 alloy in an outdoor coastal environment. [15]

tests, the stress increases as the cross-sectional area reduces with crack propagation, whereas for constant displacement tests, the stress decreases due to stress relaxation as the crack lengthens. Creep also decreases the stress by relaxation of residual stresses and those caused by applied displacements.

Wei et al.[108] in constant displacement tests of Mg-9Al (and Mg-9Al alloys containing various additions of RE, Zn and Ca), found that Mg-9Al had a threshold strain value of 0.35 % in a solution of 3.5 % NaCl + 2 % K2CrO4, and higher thresholds were measured for the alloys containing the various additions of RE, Zn and Ca. These results may indicate that plastic deformation is required for SCC, or alternatively may simply reflect that constant deflection tests may give threshold values higher than in constant load tests.

The role of strain in SCC has been attributed to the rupture of any surface film, to allow *H* ingress, or to allow localised dissolution. Wearmouth et al.[85] investigated the influence of strain rate for high-purity extruded Mg-7Al in an aqueous 2 % K_2CrO_4 + 3.56% NaCl solution. They proposed that the SCC crack propagation velocity was defined by the balance between corrosion inhibition by the film growth rate and bare metal exposure by the (crack tip) strain rate. Consequently, SCC occurred in a limited range of strain rates, where the strain at the crack tip was sufficient to overcome repassivation. This balance is the basis for the film rupture mechanism for crack initiation, which is described later (see Sec. 4.1.2).

Chakrapani and Pugh[89] reported that high-purity Mg-7.5Al exhibited reduced ductility, which is characteristic of SCC/HE, when exposed to gaseous *H* or cathodically-generated *H* in 4 wt%NaCl + 4.0 wt%K_2CrO_4 under load. Figure 20 shows that the difference in tensile properties for pre-exposed and vacuum annealed specimens was dependent on strain rate. At low strain rates there was a large difference in the UTS and elongation of the annealed and pre-exposed specimens. The fracture surfaces at the higher strain rates were completely dimpled, suggesting that ductile tearing was the dominant failure mechanism. The authors proposed that, at the higher strain rates, insufficient time was available for *H* diffusion. For the specimens tested at the slower strain rates, the difference in UTS and elongation to failure of the annealed and pre-exposed specimens was attributed to loss of *H* during annealing.

Ebtehaj et al.[107] investigated the influence of strain rate on SCC susceptibility for cast Mg-9Al. They proposed that the SCC mechanism involved diffusion of cathodically generated *H*, and that the SCC susceptibility is defined by opposing effects relating to *H* ingress as related to the proposal of Wearmouth et al.[85] It was proposed that at low strain rates, film integrity was maintained preventing *H* ingress such that ductile fracture ensued. As the strain rate was increased, the effectiveness of repassivation was reduced, allowing *H* to ingress more freely. At high strain rates, ductile tearing occurred before embrittlement, because insufficient time was available for *H* ingress. This agreed with the work by Chakrapani and Pugh.[89] Maximum susceptibility occurred at an intermediate strain rate as shown in Figure 21. Furthermore, the strain rate corresponding to maximum susceptibility was dependent on the balance between active and passive corrosion processes (as defined by the ratio of chloride and chromate ion concentrations) with this effect becoming less significant at high strain rates. As the chromate concentration increased, the tendency for repassivation was increased, so higher strain rates were required to overcome repassivation and the overall resistance to cracking increased. This explains the locations of the mimima with respect to strain rate for the curves representing 5, 20 and 35 g/L K_2CrO_4 concentration.

Nozaki et al.[91] studied SCC of AZ31B in distilled water and in NaCl solutions for various strain rates. SCC susceptibility was quantified by an SCC susceptibility index, I_{SCC}, given by

$$I_{SCC} = \frac{(E_{oil} - E_{SCC})}{E_{oil}} \times 100 \quad (11)$$

where E_{SCC} and E_{oil} were the areas under the stress-strain curves in the SCC solution and in oil, respectively, the latter

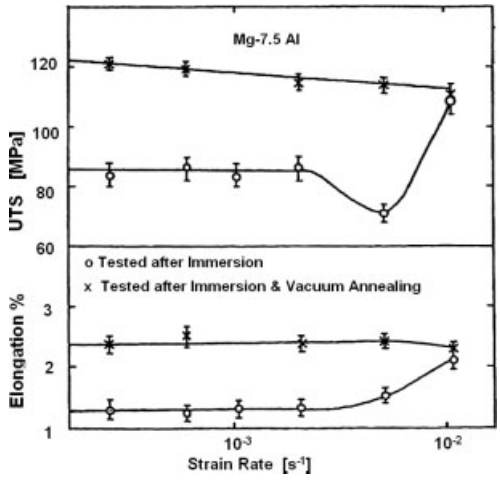

Fig. 20. Effect of strain rate on tensile properties for pre-exposed and vacuum annealed Mg-7.5Al specimens. [89]

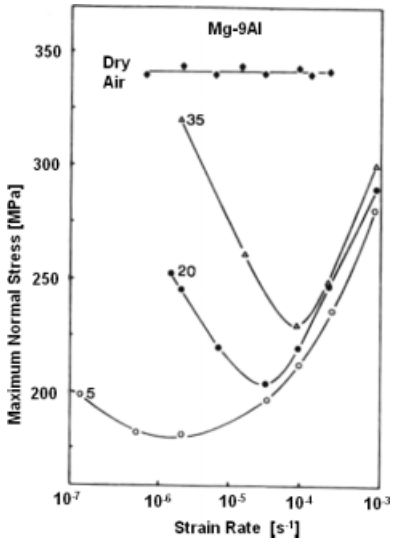

Fig. 21. Effect of strain rate on SCC susceptibility for 5, 20 and 35 g/L K_2CrO_4 and 5 g/L NaCl. [107]

being inert. I_{SCC} is high for systems with high SCC susceptibility whereas I_{SCC} tends to zero for systems with low susceptibility. Figure 22 shows that susceptibility in distilled water increased from 0 to 85 % as the strain rate was decreased from 8.3×10^{-4} s^{-1} to 8.3×10^{-7} s^{-1}. For NaCl concentrations of 4 and 8 %, susceptibility was around 90%, independent of strain rate.

Makar et al.[83] showed that the SCC velocity was dependent on the applied loading rate. For RS Mg-1Al and RS Mg9Al, the overall and SCC velocities were determined by dividing the total crack length and the SCC crack length by the test duration respectively. A greater vertical separation between overall and SCC crack velocities for a given loading rate indicated decreased SCC susceptibility. Markar et al indicated, Figure 23, that the overall and SCC crack velocities became increasingly separate, indicating that ductile tearing became increasingly dominant, as the loading rate increased from 4.8×10^{-3} mm.s^{-1} to 8.9×10^{-3} mm.s^{-1}, above which the fracture surfaces were mostly ductile.

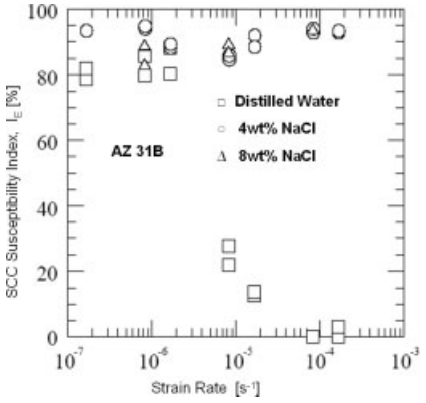

Fig. 22. Effect of strain rate on SCC susceptibility index for AZ31B in distilled water and NaCl solutions. [91]

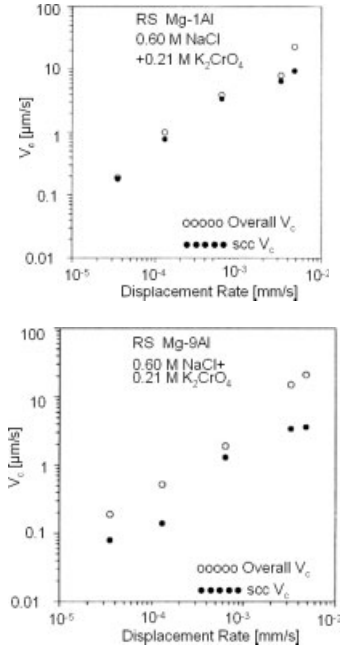

Fig. 23. Overall and SCC velocity for (a) RS Mg-1Al and (b) RS Mg-9Al in 0.21 M K_2CrO_4 + 0.6 M NaCl at various applied displacement rates. [83]

3.3. Environment Influences

This review focuses on environments pertinent to likely service for Mg alloys. However, it is also worth noting that Mg alloys have shown SCC in gaseous *H*,[89,107] these studies in gaseous *H* have been related to the SCC mechanism.

3.3.1. Air/Atmosphere

Dry air is generally considered inert for pure Mg,[71,75,76] albeit SCC has been reported in damp and outdoor air atmospheres. Pelensky and Gallaccio[81] reported that all AZxx alloys failed under outdoor exposure, including marine and rural air environments, with susceptibility increasing with periods of rain, humidity or high temperature. For indoor air at ambient temperatures, AZ61 alloy was susceptible to SCC at 98 to 100 % relative humidity. Increasing the O_2 or CO_2 concentration in the air decreased the critical relative humidity for AZ61 to 95 %. If the relative humidity was near 100 %, increasing the concentration of SO_2 and CO_2 decreased the time to cracking. Pelensky and Gallacio reported that the alloy M1 (Mg-1.2Mn) was immune to SCC in marine air environments. Kiszka[106] reported that SCC occurred for rapidly cooled Mg-14Li base alloys containing 1 % or 1.5 % Al in humid air environments. Loose and Barbian[15] reported SCC of AZ61 in annealed and as-rolled conditions in rural and coastal air atmospheres.

Marrow et al.[109] induced "SCC" in air in the cast Mg alloy WE43 in the T6 peak aged condition. Crack initiation was observed at relatively high stresses and was attributed to the cracking of an intergranular intermetallic due to its inability to accommodate the (locally) high plastic deformation of the (α) matrix. Propagation occurred in a TG manner if the crack was sufficiently long. Non-propagating cracks were observed at lower stresses on the smooth specimens, reminiscent of those reported by Wearmouth et al.[85]

3.2.2. Composition of Aqueous Solutions

The vast majority of the literature on Mg has dealt with SCC in aqueous solutions containing chloride and chromate ions in approximately equal concentrations. Chromate ions inhibit general corrosion by promoting protective film growth. Chloride ions promote film breakdown and *H* evolution, which facilitate SCC.[83,85,107] Thus, varying the ratio of chloride to chromate ions changes the balance of active and passive processes on which SCC characteristics depend.

Ebtehaj et al.[107] investigated the influence of chloride and chromate ion concentration on TGSCC susceptibility of homogenized fine-grained cast Mg-9Al. The specimens were

tested under monotonically increasing strain, constant strain and constant load in chloride-chromate solutions. The threshold stress or threshold stress intensity factor (depending on whether the specimen was plain or notched) was a minimum when the ratio of chloride ions to chromate ions was approximately 1-2 (see Fig. 24). The authors proposed that the role of chromate was to increase the open circuit potential, and therefore the pitting potential, for a given chloride concentration. SCC required a balance between active and passive corrosion behavior: chromate-only solutions result in complete passivity preventing pitting which was essential for *H* ingress, whereas chloride-only solutions result in excessive general corrosion which could outrun crack growth. Thus, maximum susceptibility occurred at intermediate chloride/chromate ratios. This was contradicted by Pelensky and Gallaccio[81] who stated that susceptibility of AZ61 increased as the concentration of K_2CrO_4 was increased from 3 to 200 g/L in 35 g/L NaCl solution and, similarly, susceptibility also increased as the concentration of NaCl was increased from 40 to 200 g/L in 5 g/L K_2CrO_4 solution.

Makar et al.[83] found that for rapidly solidified and as-cast Mg-1Al and Mg-9Al in NaCl-only solutions, SCC occurred in a limited range of relatively high strain rates and not at all in K_2CrO_4-only solutions. The requirement for a relatively high strain rate coupled with the trends outlined by Ebtehaj et al.[107] suggested that HE is dependent on the localisation of dissolution and *H*-evolution reactions by appropriate chloride-chromate ratios. Varying the chloride-chromate ratio varied the strain rate at which localisation occurred (see Fig. 21). The relationship between strain rate and environment varies with system. Nozaki et al.[91] reported no significant variation in the SCC susceptibility index (see Eq. 11) for strain rates between 8.3×10^{-5} s^{-1} and 8.3×10^{-7} s^{-1} for NaCl-only solution with concentrations between 2 and 8 % but did find an increase in susceptibility index from 0 to 85 % for distilled water (see Fig. 25).

SCC in other aqueous solutions has also been reported. Fairman and West[92] found that immersion of single-phase

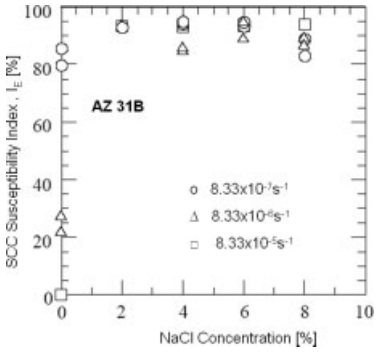

Fig. 25. Effect of NaCl concentration on SCC susceptibility (quantified according to Equation 13). [91]

Mg-6.5Al in NaCl + $K_2Cr_2O_7$ solution resulted in a lower threshold stress than for NaCl + K_2CrO_4 solution (see Fig. 26). Speidel et al.[105] reported that crack growth in distilled water was accelerated by additions of sulfate or bromide ions as shown in Figure 12.

Fairman and Bray[110] tested pure Mg and various Mg-Al, Mg-Al-Fe and Mg-Al-Zn alloys, heat treated to ensure TGSCC, in a 4 wt%NaCl + 4 wt%Na_2CrO_4 solution. They found that additions of $NaNO_3$ or Na_2CO_3 to the solution improved the ability to repair faults in the surface film. Such faults would otherwise contribute to SCC by allowing chloride ion penetration and tunneling (see Sec. 4.2.1). This also increased the thickness and stability of the film and made the corrosion potential less negative. The inhibition of SCC for Mg-6Al alloys in chloride-chromate solutions by NO_3^- ions was also investigated by Frankenthal[111] who proposed that NO_3^- ions prevent breakdown of the chromate-produced film by chloride ions. Frankenthal observed that the unstressed specimens in 4 % NaCl + 4 % K_2CrO_4 solutions were subject to profuse pitting, however with the addition of 3 % $NaNO_3$, pitting was only slight. Furthermore, the addition of nitrate to the chloride-chromate solution resulted in a more positive corrosion potential, similar to that for a chromate-only solution.

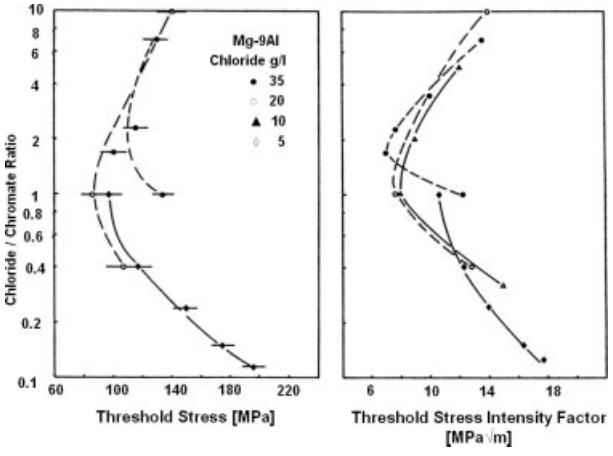

Fig. 24. Effect of chloride-chromate ratio on SCC susceptibility as characterized by threshold stress (plain specimens) or threshold stress intensity factor (notched specimens). [107]

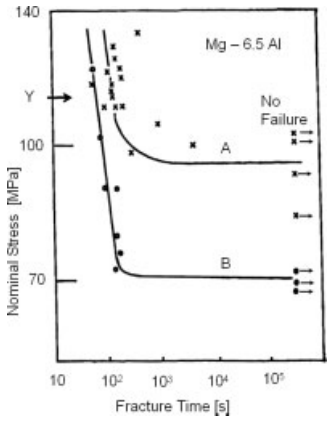

Fig. 26. Variation in fracture time with applied stress for single-phase Mg-6.5Al alloy in 4 wt%NaCl + 4 wt%K_2CrO_4 (chloride-chromate) (A) and 4 wt%NaCl + 4 wt%$K_2Cr_2O_7$ (chloride-dichromate) (B) solutions. [92]

Timonova[74] stated that MA3 alloy was susceptible to SCC in sodium carbonate solution, with susceptibility constant for concentrations between 0.005 and 0.15 *N*, and increasing with concentrations between 0.15 and 1.0 *N*.

An extensive assessment of environmental influences was carried out by Pelensky and Gallaccio[81] for pure Mg and Mg-Mn, Mg-Al, Mg-Al-Zn, Mg-Zn-Zr, Mg-Al-Mn and Mg-Li alloys in air, water and numerous aqueous solutions. Most alloy-environment combinations resulted in SCC. The following general trends were noted:

- High purity Mg and Mg-2Mn failed in KHF_2.
- Mg-5Al failed in distilled water.
- ZK60A-T5 (Mg-5.5Zn-0.45Zr) failed rapidly in distilled water and sea water.
- ZK60A-T5 stressed to 90 % of its yield strength failed rapidly in KCl, CsCl, NaBr, NaCl and NaI solutions.
- AZ61 failed in Na_2CO_3 solution with susceptibility constant for concentrations between 0.265 and 15.9 g/L and increasing with concentration between 15.9 and 53 g/L.
- AZ61 did not fail in K_2CrO_4 + $NaCH_3COO$, K_2CrO_4 + Na_2CO_3 or K_2CrO_4 + $NaNO_3$ solutions.
- AZ61 was susceptible in NaCl + K_2CrO_4, K_2CrO_4 + Na_2SO_4, Na_2SO_4, $NaNO_3$, Na_2CO_3, NaCl, $NaCH_3COO$ (in order of decreasing susceptibility).
- The susceptibility of AZ61 and Al-1.5Mn in NaCl solutions increased with solution concentration.

Little explanation of these trends was offered by the authors. Many of the environments were selected to represent common service conditions, but it was noted that accelerated SCC tests should not be used to predict service lifetimes, because of the large number of metallurgical, environmental and mechanical variables involved, and that accurate lifetime prediction requires accurate simulation of service conditions.

Yakovlev et al.[112] found that MA2 exhibited similar SCC kinetics in Na_2SO_4 + NaOH solution as in NaCl + $K_2Cr_2O_7$ solution. Tomashov and Modestova[97] also stated that, for Mg-Mn alloys, similar corrosion characteristics and SCC failure times were observed for Na_2SO_4 and NaCl solutions of equal concentration. Marichev et al.[113] stated that NaOH was associated with passivation of Mg alloys. Timonova[74] showed that MA3 was susceptible to SCC in H_2SO_4 solution, with susceptibility increasing with solution concentration, to some maximum, and then decreasing with further increase in concentration as general corrosion became more profuse.

Timonova[74] examined the resistance of Mg-8Al to SCC and general corrosion in 0.01 *N* solutions of NaCl, HCl, HNO_3, NaOH, NaF and HF. Figure 27 and Figure 28 show, that for NaF, general corrosion (quantified by weight loss) was limited by the formation of a dense surface film, which also inhibited the occurrence of SCC (quantified by time preceding cracking), whereas for NaOH, general corrosion was also limited although SCC occurred, which was attributed to a less dense surface film. For HCl and NaCl, the general corrosion rate was high, preventing SCC. Perryman[90] observed SCC failures of Mg-5Al in saturated magnesium carbonate, 0.5 % potassium fluoride, 0.5 % potassium hydrogen fluoride and 0.5 % hydrofluoric acid (in order of decreasing time to failure).

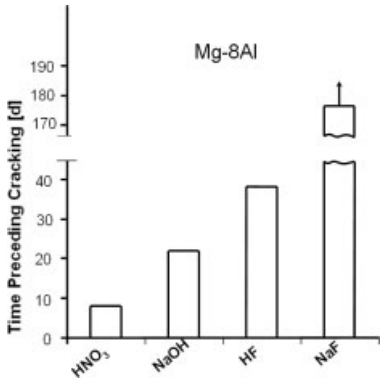

Fig. 27. SCC susceptibility of Mg-8Al in various aqueous solutions. [74]

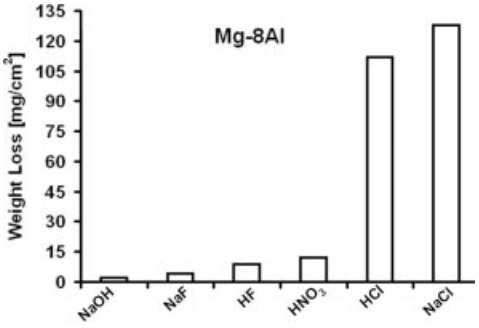

Fig. 28. General corrosion susceptibility of Mg-8Al in various aqueous solutions. [74]

KHF_2 solutions appear to cause SCC in most alloys including high purity Mg and the Mg2 %Mn alloy.[114] Since the F^- ion is an inhibitor for the corrosion of Mg by the formation of a fluoride film, at least part of the electrochemical explanation may lie in film breakdown and repair kinetics.

3.3.3. Electrochemical Potential

It is generally believed that cathodic polarization retards, and anodic polarization accelerates, SCC in Mg alloys.[16] Stampella et al.[75] proposed that for pure Mg in a 10^{-3}M Na_2SO_4 solution under open circuit conditions, SCC was invariably preceded by pitting, and it was demonstrated that the open circuit corrosion potential (–1.36 V) coincided with the pitting potential. Anodic polarization to –1.16 V resulted in more severe pitting and greater susceptibility to cracking. Cathodic polarization to –1.5 V and –2.5 V resulted in a more stable film and prevention of pitting. It was also shown that, at the more cathodic potentials, repassivation was sufficient to overcome mechanical film rupture by strain rates as high as 5.7×10^{-6} s^{-1}. That SCC in Mg alloys can be prevented by cathodic polarization has also been demonstrated by Priest

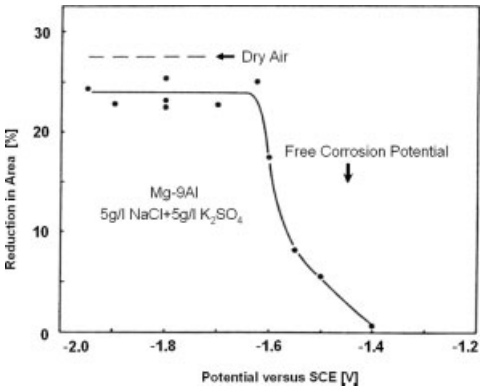

Fig. 29. Influence of applied potential on reduction in area for Mg-9Al subject to a strain rate of 2×10^{-6} s^{-1} in 5 g/L NaCl + 5 g/L K_2CrO_4 solution. [107]

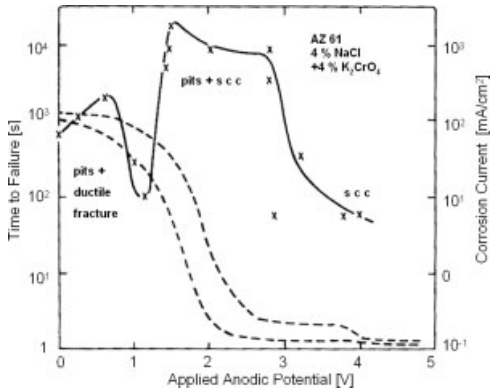

Fig. 31. Variation in failure time, t_f, with applied anodic potential for AZ61 in 4 wt% NaCl + 4 wt% K_2CrO_4 (dashed line indicates corrosion current). [94]

et al.[80] and Logan.[115] Ebtehaj et al.[107] demonstrated that SCC susceptibility (characterized in Fig. 29 by reduction in area) decreased rapidly with decreasing applied potential. Below approximately –1.6 V the reduction in area was constant and approximately equal to that for dry air.

Fairman and Bray[110] showed that for various 2-phase Mg-Al and Mg-Al-Zn alloys, heat treated for 1 h at 400 °C to ensure TGSCC, over a broader range of applied anodic potentials, the relationships between polarization and SCC susceptibility was more complex than suggested by Stampella et al. They investigated the effects of applied potential on Mg-Al alloys, heat treated to ensure TGSCC, in chloride-chromate solutions. Figure 30 shows that, for potentials from the open circuit up to ~1 V, such as at position "x", the corrosion current was high and there was rapid SCC. At potentials ~1.8 V, such as at position "y", there was excessive film breakdown such that general corrosion prevented SCC. (That is, the rate of general corrosion exceeded the rate of SCC). Film breakdown and SCC occurred at potentials such as at position "z". SCC was retarded by passive film formation at applied potentials greater than ~3.8 V.

In a subsequent study, Fairman and Bray[94] showed that two-phase AZ61 and AZ80 alloys, heat treated to induce IGSCC, were influenced differently by applied potential, reinforcing the view that the SCC mechanism for IGSCC is different to that for TGSCC. Figure 31 shows that, for AZ61, failure could occur due to pitting, such as at low applied potentials, or SCC, such as at high applied potentials, or by some combination of these two mechanisms. At high applied anodic potentials the electrochemical SCC mechanism was uninhibited because passive film formation was negligible. At lower potentials cracking was preceded by pitting resulting in delayed crack initiation. As the applied potential was reduced further, failure was dominated by pitting which reduced the cross-sectional area sufficiently to induce ductile tearing. Similar relationships also occurred for AZ80 as shown in Figure 32.

The influence of applied potential on the SCC velocity in Mg alloys was investigated by Marichev and Shipilov.[113] They showed that, for various alloys containing Al, Zn, Mn and RE in NaCl solutions, cathodic polarization decreased and anodic polarization increased the crack velocity. These trends were attributed to the alkalization and acidification of the crack tip solutions leading to film stabilization and breakdown respectively. It was also shown that, for the high-strength Mg-7.6Y-1.7Zn-1.5Cd-0.3Zr alloy in passivating solu-

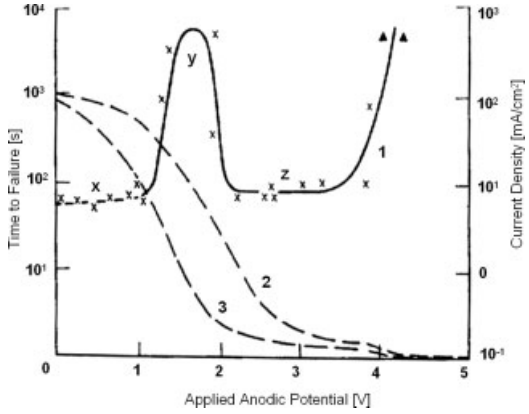

Fig. 30. Variation of time to failure with applied anodic potential for AZ61 and AZ80 in 4 wt% NaCl + 4 wt% K_2CrO_4. Dashed lines indicated maximum (2) and minimum (3) current density. Triangles indicate no SCC. [110]

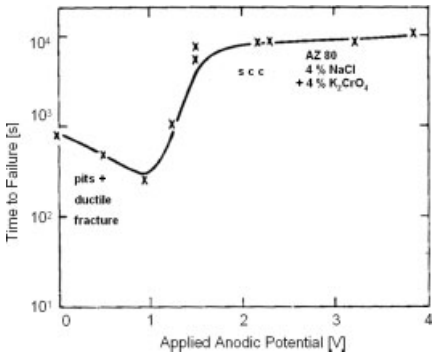

Fig. 32. Variation in failure time with applied anodic potential for AZ80 in 4 wt% NaCl + 4 wt% K_2CrO_4 solution. [94]

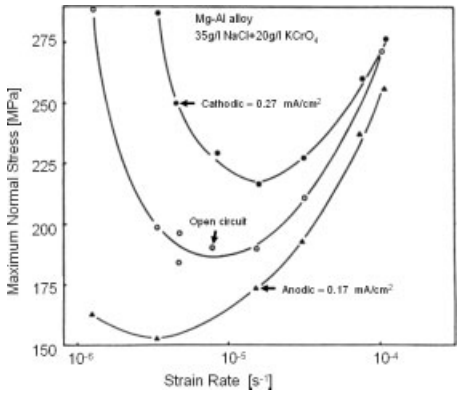

Fig. 33. Influence of strain rate on SCC susceptibility for various applied potentials. [107]

tions (1 *M* NaOH or 2 *M* CrO_3), cathodic polarization resulted in rapid acceleration of cracks.

Ebtehaj et al.[107] showed that the strain rate corresponding to maximum SCC susceptibility (the maximum nominal stress below which there was no SCC) was increased as the corrosion potential became more cathodic (see Fig. 33). This trend was attributed to the promotion of film growth by cathodic polarization such that higher strain rates were required to induce film rupture and localised corrosion.

3.3.4. pH

Reports on the influence of pH on SCC are few but those that exist agree that SCC does not occur in chloride-chromate solutions with pH values greater than 12. Sager et al.[116] reported that the time to failure for the Mg-6.5Al-1Zn alloy in a chloride-chromate solution was constant for pH values between 5 and 12. At lower pH values SCC susceptibility increased sharply with decreasing pH whereas at higher pH values SCC was inhibited (see Fig. 34). Pelensky and Gallaccio[81] stated that for AZ61 in a chloride-chromate solution, SCC occurred for pH values between 2 and 12 but not at higher pH values. It has also been established by several workers[80,94,95,] that pH has no influence on crack morphology.

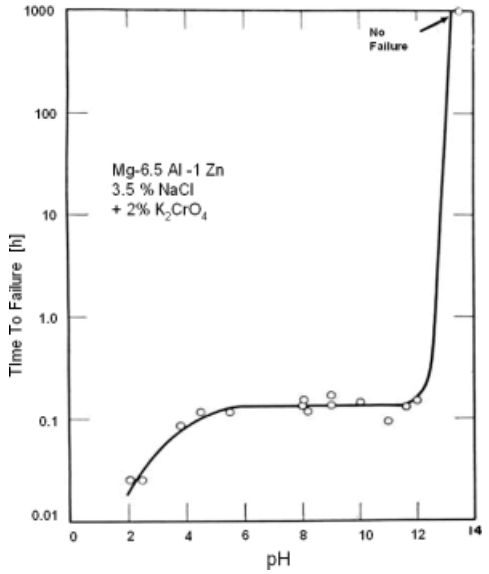

Fig. 34. Variation in time to failure with pH for Mg-6.5Al-1Zn alloy in 3.5 % NaCl + 2. % K_2CrO_4 solution. [116]

Loose[117] and Scully[114] report that, in non-fluoride solutions, SCC is inhibited at pH values greater than 10.2 This is probably related to the greater ease of film formation that occurs in highly alkaline solution. However, it is useful to remember that Timonava[74] reported SCC in 0.01 *N* NaOH.

3.3.5. Temperature

Miller[16] stated that susceptibility of Mg alloys to SCC in air and water increases with temperature. Pelensky and Gallaccio[81] reported that SCC susceptibility for AZ61 in a chloride-chromate solution was a maximum at around 40 °C whereas susceptibility of MA2 and AZ80 in H_2SO_4 + NaCl solution increased with temperature to around 70 °C. Romanov[118] also showed that SCC susceptibility increased with temperature for MA2 in a H_2SO_4 + NaCl solution, but for passivating environments, increased temperature decreased SCC susceptibility due to improved passivation. Increasing temperature also increases the amount of creep, which may cause stress relaxation resulting in improved SCC resistance or may contribute to film rupture resulting in reduced SCC resistance.

4. SCC Propagation Mechanisms

SCC in Mg alloys has been generally attributed to one of two groups of mechanisms: continuous crack propagation by anodic dissolution at the crack tip, Figure 1, or discontinuous crack propagation by a series of mechanical fractures at the crack tip, Figure 2.[16,75] Dissolution mechanisms include preferential attack, film rupture and tunneling whilst mechanical mechanisms may include cleavage and HE. It appears that there are different mechanisms for IG and TG crack propagation. For IGSCC there is a common view that the dominant mechanism is preferential anodic dissolution of the metal matrix immediately adjacent to cathodic grain boundary precipitates, Figure 10. For TG cracking it appears that dissolution mechanisms such as film rupture and tunneling cannot explain the commonly observed crack propagation rates and fracture surfaces (particularly the interlocking fracture surfaces observed by Pugh and co-workers[14,86,88,89] for opposing fracture surfaces) and there is considerable evidence to support HE induced cleavage. *H* induced plasticity may also play a role, particularly to produce the fracture surfaces reported by Lynch and Trevena[71] which had concave features on both opposing fracture surfaces, Figure 6.

It is widely believed that there is a threshold, σ_{SCC}, below which SCC does not occur,[11,12,114] and it has been suggested[85] that σ_{SCC} is related to the yield stress. In single crystals, it has been reported[119] that the yield strength point must

be exceeded to produce plastic deformation and this has been observed to be necessary for SCC. However, it is useful to note that Table 2 indicates that σ_{SCC} is significantly less than the yield stress for many alloy-environment combinations.

4.1. Dissolution Mechanisms

4.1.1. Preferential Attack

The preferred model for IGSCC in Mg-Al alloys (see Fig. 10) is accelerated dissolution of the metal matrix adjacent to $Mg_{17}Al_{12}$ grain boundary precipitates, which precipitate during slow cooling of alloys with Al concentrations greater than 2.1 %.[94] Cracking was thought to be initiated by preferential dissolution of the metal matrix resulting in the precipitate being left proud of the surface, causing stress concentration and faulting of the $Mg(OH)_2$ film.[94] Thus, crack initiation and propagation are thought to be driven by the potential difference between $Mg_{17}Al_{12}$ and the Mg-Al matrix, which Fairman and Bray[94] reported to be around 300 mV. Stress pulls apart opposite crack surfaces and allows migration of species to the crack tip. Pardue et al.[95] showed that this mechanism is continuous (assuming a continuous grain boundary precipitate) as indicated by a lack of noise signals in acoustic emission studies. Fairman and Bray[94] reported some discontinuities in the extension of IGSCC specimens, attributing them to the intersection of unfavorably oriented grains.

A similar mechanism would be expected for other alloy systems, because most second phases tend to accelerate the corrosion of the adjacent magnesium matrix.

An upper estimate of the crack velocity for this mechanism can be made based on the recent quantitative study of the galvanic corrosion of the (high-purity) magnesium alloy AZ91D[34] coupled to steel. It was found that the corrosion penetration rate was ~0.69 m/y or 2.2×10^{-8} m/s for the Mg alloy immediately adjacent to the steel. The penetration rate could be orders of magnitude higher for a low purity alloy. This estimated penetration rate must be considered an upper estimate, because the potential difference driving the galvanic corrosion for a Mg-Steel couple is considerably higher than the potential difference of 300 mV between the potentials of the α and β phase in an Mg-Al alloy.

4.1.2. Galvanic Attack by Film Rupture

Logan[115,120] proposed an alternative electrochemical mechanism for AZ31. He postulated that, when the surface film is ruptured by an applied strain rate, an electrochemical cell occurs between the anodic film-free area and the cathodic filmed area. The potential difference between the anode and cathode was estimated to be 0.24 V so that rapid localised dissolution could occur at the exposed substrate resulting in crack initiation. Stress concentration at the crack tip was thought to prevent the film from reforming such that crack propagation is continuous as shown in Figure 1. Miller[16] stated that, for film rupture models, continuous crack growth is possible only where repassivation is insignificant, otherwise there is discontinuous crack growth by alternating phases of film rupture and repassivation. That crack growth is defined by the competing rates of film rupture and regrowth was also proposed by Ebtehaj et al.[107] and Wearmouth et al.[85]

Logan's hypothesis[115,120] that the SCC mechanism was entirely electrochemical was based on the observation that cathodic polarization could prevent the occurrence of SCC. However, HE models generally require the exposure of film-free surfaces, which may also be prevented by cathodic polarization. Furthermore, Logan calculated from Faraday's law that the observed crack propagation rates (10×10^{-6} m/sec) required an effective current density of 14 A/cm^2. Similarly Pugh et al.[121] observed crack velocities between 6×10^{-6} and 40×10^{-6} m/sec for Mg-7.6Al alloy in a chloride-chromate solution, which correspond to current densities between 8.05 and 57.5 A/cm^2. Such current densities were considered by Pugh et al to be prohibitively high for a dissolution model.

Logan did not report on any microstructural or fractographic examination and it is known that AZ31 may contain $Mg_{17}Al_{12}$ precipitates.[94] Logan may have been observing IG failure caused by the preferential attack mechanism (see Sec. 4.1.1).

4.1.3. Tunneling

The tunneling model was introduced by Pickering and Swan.[122] They proposed that film rupture at emerging slip steps causes localised electrochemical cells, resulting in the formation of tubular pits. The direction of these pits was thought to be initially defined by the electrochemical potential difference between the metal matrix and the fine precipitates (assumed to be $Mg_{17}Al_{12}$) which occur on slip planes. Subsequently, once a local electrochemical cell capable of preventing film repair and sustaining enhanced anodic dissolution is established at the crack tip, propagation was thought to continue independent of the precipitate. Crack extension occurs by ductile tearing of the narrow ligaments of metal between parallel tunnels as illustrated in Figure 35. Ductile tearing destroyed the local cells at the crack tips so new pits were formed in order for the process to repeat.

Unlike the film rupture model, Pickering and Swan claim that the current density required to achieve the observed crack penetration rates are realistic. However, the interlocking fracture surfaces often observed for TGSCC cannot be readily explained by this model. Furthermore, Pickering and Swan proposed this mechanism for both Mg-1Al and Mg-7Al but it is unlikely that there are $Mg_{17}Al_{12}$ precipitates in the former alloy which has only 1 % Al.

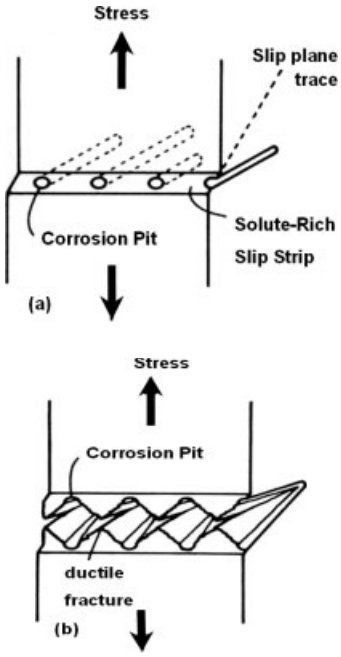

Fig. 35. Tunneling model for SCC. (a) Tubular pits form due to film rupture on slip steps. (b) Crack propagation occurs by ductile tearing of remaining ligaments. [122]

4.2. Mechanical Fracture Mechanisms

4.2.1. Cleavage Fracture

The most commonly proposed mode of TGSCC of Mg alloys is discontinuous cleavage. Most Mg alloys have HCP crystal structures, which are susceptible to cleavage due to the lack of slip systems.[123] Cleavage is usually evidenced by fluctuating acoustic emissions and corrosion potentials, and by faceted, interlocking fracture topographies. Various reasons for embrittlement not involving *H* ingress have also been proposed and are discussed in this section.

The majority of cleavage models involve alternating stages of electrochemical attack and mechanical fracture. The first of these by Pardue et al.[95] suggested that transgranular cracking in AZ61 alloy is initiated by highly localised corrosion pitting. High stress concentration at a corrosion pit may induce a cleavage crack, which propagates within the grain until some obstruction, such as a grain boundary, is intercepted. The obstruction is subsequently removed by further electrochemical attack and the process is repeated. The alternating electrochemical and mechanical stages were evidenced by discrete acoustic emissions and corrosion current fluctuations respectively; although, Pardue et al admitted that this was insufficient to propose a definitive cracking mechanism. The occurrence of brittle fracture was attributed to dislocation blocking, and thus inhibition of plastic deformation, by FeAl precipitates within grains or to lattice distortion by Fe ions providing the activation energy for magnesium dissolution.

Fairman and West[92] elaborated on this model by proposing that pitting is initiated by film rupture due to basal slip and that continued film rupture at the base of the pit causes it to deepen by ~0.1-0.2 μm. Stress concentration at the base of the pit initiates cleavage on whichever cleavage plane, (0001), $(10\bar{1}0)$ or $(10\bar{1}1)$, is most normal to the tensile axis, as evidenced by a stepped fracture surface with wide forward steps in the cracking plane. The width of the steps was correlated with changes in longitudinal extension of the specimens. After limited propagation, the crack arrests due to stress relief, cross slip of dislocations, or interference by precipitates or flaws. The process is repeated when slip occurs again at the crack tip resulting in the formation of another pit. The crack changes orientation at grain boundaries; however, since there are multiple cleavage planes it still propagates roughly perpendicular to the tensile axis. Ductile failure finally occurs when the cross section of the specimen is reduced such that the ultimate tensile stress is reached. Fairman and West also acknowledged the electrochemical stage in crack propagation, based on observations that cracking could be stopped at any time by cathodic polarization. They also concede that film rupture is unnecessary where severe localised corrosion, due to $Mg_{17}Al_{12}$ grain boundary precipitates, occurs.

Pugh et al.[121] criticized Fairman and West's model for inadequately explaining why stress intensification at the immerging pit initiates cleavage, rather than ductile fracture, or why the cleavage crack stops, in spite of the fact that the stress intensity factor increases with crack length. Instead, Pugh et al proposed a variation of the film-rupture model for transgranular cracking by adding that embrittlement of the metal immediately ahead of the crack tip occurs by the formation of a porous surface layer of an oxide (other than MgO) or selective dissolution of Mg or Al, and that crack arrest is due to the blunting of the crack tip as it enters the ductile substrate ahead of the embrittled layer. Thus, the characteristic alternating stages were proposed to be: embrittlement of a thin surface film, film rupture, crack propagation, and crack arrest. This model was also supported by crack propagation velocities, measured using a traveling microscope to be ~5.8 to 42 × 10^{-6} m/s (0.35-2.5 mm/min), which Pugh et al proposed could only be explained by a mechanism involving a fast mechanical stage. The embrittling surface film was speculated to be an oxide or a de-alloyed later. HE was rejected based on observations that cracking is retarded and accelerated by cathodic and anodic polarization respectively; however, this effect of polarisation has since been commonly attributed to the negative difference effect.

The cleavage model proposed by Pugh et al.[121] was disputed by Fairman and Bray[110] on two accounts. Firstly, they observed no fractographic evidence of brittle fracture for Mg-Al alloys in chloride-chromate solutions. Secondly, they detected no oxide layer on the fracture surfaces. Fairman and Bray instead proposed a ductile fracture model as evidenced by striations perpendicular to the crack propagation direction, which were attributed to positions of successive crack arrest. This ductile fracture interpretation conflicts with the majority of fractographic evidence provided by other workers

for mechanical fracture mechanisms. Fairman and Bray stated that for Mg-Al alloys, Al^{3+} ions displace Mg^{2+} ions in the $Mg(OH)_2$ surface film, requiring vacancies in the film lattice to preserve electroneutrality. This increased the susceptibility of the surface film to localised rupture. Film rupture was thought to occur by a flow of dislocations causing slip in the metal and failure on the film basal plane. Chloride ions migrate to regions of high tensile strain; therefore tunneling occurs at the rupture site if dislocation concentration is sufficient to overcome repassivation (see Fig. 36). Stress concentration at the tip of the tunnel would then lead to ductile tearing (as shown in Fig. 37) until the crack is relaxed by plastic flow. Since Mg-Al has multiple slip systems a new tunnel may then be created at the crack tip and the process is repeated.

Pardue et al.[95] and Chakrapani and Pugh[86] showed that stages of crack propagation coincided with discrete spikes in acoustic emission measurements. Unstressed specimens in solution emitted a steady acoustic signal, which was associated with *H* evolution from pitted areas whilst specimens undergoing plastic deformation in air emitted no signal. Stressed specimens in solution emitted discrete acoustic signals superimposed onto the continuous "*H*" signal, indicating discontinuous crack advance. Pardue et al also observed that the electrochemical step in the cracking process corresponded with fluctuations in corrosion currents, due to the repeated exposure of fresh anodic metal.

Chakrapani and Pugh[86] determined from measurements of the distance between acoustic emission "spikes" that the average crack velocities in Mg-7.6Al were between 5 and 30 × 10^{-6} m/s. Similarly, using a moving microscope Pugh et al.[121] determined that, for the same alloy, average crack velocities were between 6 and 40 × 10^{-6} m/sec. Such velocities could not be reconciled with dissolution models according to Faradays law, adding further support to a mechanical fracture model.

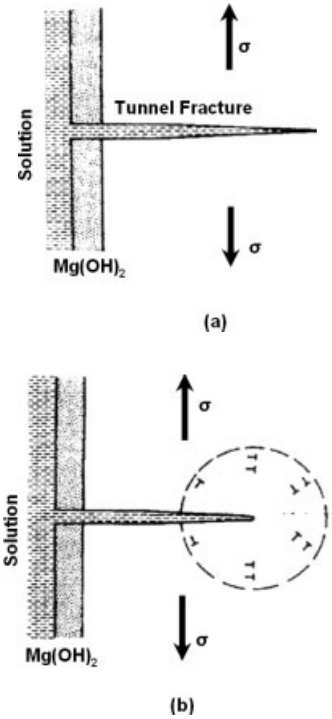

Fig. 36. (a) Propagation of crack by ductile fracture from corrosion tunnel. (b) Crack arrest by stress relaxation resulting in plastic deformation. [110]

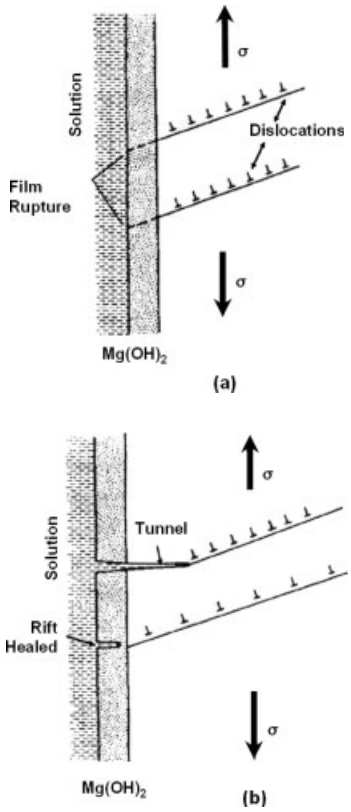

Fig. 37. (a) Dislocation flow causes film rupture. (b) Corrosion tunnel forms by attack at moving dislocations. [110]

Various workers[14,72,86,88] have reported that TGSCC in Mg alloys results in fracture surfaces consisting of flat, parallel facets separated by perpendicular steps, consistent with a cleavage mechanism. The steps and facets are generally parallel to the direction of crack propagation and change direction at grain boundaries.[72] Opposite fracture surfaces are matching and interlocking, which is also consistent with the occurrence of cleavage and is difficult to explain by a dissolution model.[14] The fracture surfaces show numerous jogs resulting from overlap of parallel cleavage cracks (see Fig. 38) further evidencing discontinuous propagation. Reports on the crystallography of these surfaces are generally inconsistent and Meletis et al attributes this to the common use of two surface analysis methods rather than more accurate photogrammetric methods. That there can be a ductile component of the fracture mechanism was shown by Lynch and Trevena[71] who observed concave features on opposing fracture surfaces for higher crack propagation velocities, such that the opposing fracture surfaces were not interlocking.

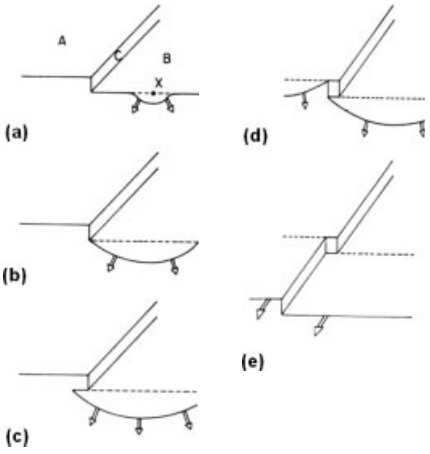

Fig. 38. Jog formation during discontinuous cleavage. After arrest the crack reinitiates at X (a) and advances on facet B (b). The crack overshoots the cleavage step (c) resulting in jog formation by secondary cleavage (d) and finally advances uniformly. [86]

4.2.2. Hydrogen Embrittlement (HE)

The most commonly cited mechanism for SCC in Mg alloys is HE; however, specific mechanisms to explain crack propagation rates and fracture surface topography in terms of *H* ingress are few. Possible mechanisms include *H* enhanced decohesion (HEDE), *H* enhanced localized plasticity (HELP), Adsorption-induced dislocation emission (AIDE) and formation of brittle stress-induced hydrides at the crack tip.

On first blush, HE might seem an unlikely mechanism: cathodic polarization might be expected to increase *H* evolution but has been shown to retard cracking whereas anodic polarization might be expected to decrease *H* evolution and has been shown to accelerate cracking.[16,75,107] This contradiction was explained in terms of the negative difference effect (see Sec. 2.1) by Ebtehaj et al.[107] who showed that large amounts of *H* were evolved within a discrete range of anodic polarization. Ebtehaj et al supported the *H*-ingress mechanism for SCC in Mg-Al alloys by correlating test results for cast Mg-9Al stressed in dry gaseous *H* and in chloride-chromate solutions. They also reported that cracking in, initially plain specimens, invariably began at regions of localised pitting and that, for slow applied strain rates, the crack initiation potential coincided with the pitting potential. Thus it has been inferred that the role of pitting is to allow *H* ingress through exposed metal surfaces.

Chakrapani and Pugh originally proposed that transgranular SCC for hot-rolled Mg-7.5Al in NaCl-K_2CrO_4 solution occurred by discontinuous cleavage evidenced by the stepped fracture surface topography; however, they also observed that *H* evolution invariably occurred at corrosion pits.[86,88] Subsequent work by the same authors[89] proposed that the "cleavage-like" fracture surfaces could be due to HE. It was shown that specimens that were stressed in gaseous *H* or exposed to aqueous solution prior to the application of stress exhibited a loss of ductility and cleavage-like fracture surfaces. This proposal was further evidenced by inert gas fusion methods which showed that the *H* concentration of the specimens progressively increased with time, and vacuum annealing, which partially reversed the effects of *H* exposure (see Fig. 20). Furthermore the occurrence of an anodic dissolution mechanism was discounted by the experimental determination of no chloride or chromate species on the fracture surfaces.

Chakrapani and Pugh[89] inferred that the mechanism for slow crack growth was repeated cycles of *H* diffusion to the crack tip region followed by brittle fracture. This was supported by discontinuous signals observed during the acoustic emission studies. It was also suggested that the role of *H* in the brittle fracture could be in the formation of brittle hydrides or to produce decohesion. They inferred that since SCC fractures tend to occur on $\{31\bar{4}0\}$ planes, these may correspond to the habit or cleavage planes of a hydride. It was observed that fracture surfaces for SCC and pure-HE systems were different: the latter tended to be flatter and without the pleated/stepped structure. It was speculated that this could be related to *H* fugacity and *H* entry kinetics, and the fact that, for SCC conditions, dissolution occurs at the crack tip.

H effects were also identified by Makar et al.[83] by correlating the results of pre-exposed and in situ tests. Differences in the fracture surfaces for the two tests were observed, suggesting that the mechanisms for samples subject to HE in the presence and absence of stress was somewhat different. This was explained in terms of the crack tip area available to *H* entry and/or the different distributions of hydrided regions with the samples. Some samples were vacuum annealed prior to testing and it was found that the environment effects were mostly reversible, as reported by Chakrapani and Pugh.[89]

Makar et al modelled the active mechanisms at various strain rates for rapidly solidified Mg-9Al in chloride-chromate solution. Crack propagation velocities for anodic dissolution, ductile tearing and HE were modeled according to Faraday's law, fracture mechanics principals and the solubility of *H* in the Mg lattice, respectively. By plotting crack velocity with respect to crack tip strain rate (Fig. 39), it was pro-

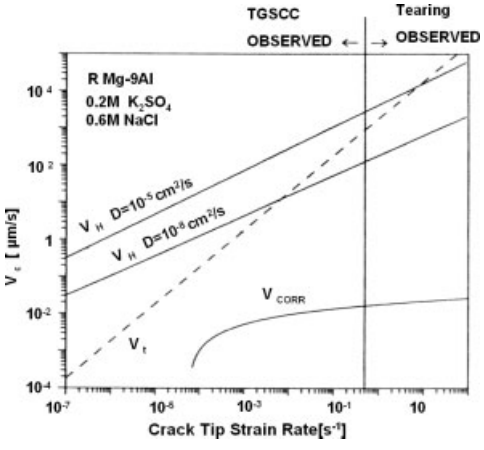

Fig. 39. The effect of crack tip strain rate (ε_{ct}) on crack velocities (v_c) calculated for ductile tearing (v_t), dissolution (v_{corr}) and HE (v_H). Note that v_H is given for two H diffusion coefficients. [83]

posed that HE (which was proposed to occur by the formation of Mg dihydride ahead of the crack tip) was the dominant propagation mechanism for values of crack tip strain rate less than $10^{-2}-10\ s^{-1}$ (0.5 as determined experimentally) depending on the *H* diffusivity. At higher strain rates, crack velocity due to ductile tearing overtakes and becomes the dominant mechanism. The crack velocity due to anodic dissolution is relatively insignificant for all strain rates and at some discernible strain rate repassivation prevents any dissolution from occurring.

Stampella et al.[75] studied the connection between the anodic pitting process and the cathodic cracking process for pure Mg in $10^{-3}M$ Na_2SO_4 solution, with the pH adjusted to 10.0 by NaOH additions. They proposed that for SCC to occur *H* must be evolved from film-free pit walls. Figure 5 shows that specimens anodically polarised and stressed in solution exhibited embrittlement and a reduction in tensile strength; however, these effects were mostly reversible by exposure to air at room temperature. This contradicted the suggestion of HE by the formation of high-pressure molecular *H* bubbles or by the formation of brittle hydrides, since Mg dihydride is not stable at room temperature. Instead, Stampella et al proposed the embrittlement mechanism involves atomic *H* in solid solution lowering the IG and TG cleavage strength of the Mg matrix.

Lynch and Trevena[71] identified the mechanism for SCC in pure Mg by comparing the fracture surfaces for slow and rapid crack growth in an aqueous environment, rapid crack growth in liquid alkali metals (Na, Cs and Rb) and overload crack growth in dry air. Liquid metal embrittlement was thought to occur by the adsorption of metal atoms at the crack tip at high crack velocities since insufficient time was available for other reactions to occur and the solubilities of the tested alkali metals in Mg were negligible. The authors proposed that, for stress corrosion crack velocities $\sim 5 \times 10^{-2}$ m/s in aqueous environments, HE also occurs by adsorption since insufficient time is available for localised dissolution or *H* diffusion (this is now called the AIDE mechanism[124]). They also suggested that dislocation transport of *H* is unlikely at these high crack velocities.

At low crack velocities, Lynch and Trevena proposed that *H* diffusion is likely to occur; however, adsorption was thought to still be the dominant mechanism for embrittlement. This was evidenced by the correlation between the fracture planes, crack propagation directions and fracture surfaces for LME and slow SCC fracture. It was also noted that no evidence of hydride formation was apparent on the fracture surfaces. At low crack velocities, adsorption at external crack tips could be inhibited by film formation, necessitating diffusion to and adsorption at internal cracks. The authors suggest that this could explain why HE characteristics are apparent for pre-exposed specimens.

It is important to note that the calculations by Lynch and Trevena for *H* diffusion were based on an approximate value for *H* diffusivity of $\sim 10^{-9}$ cm^2/s. This was based on hydride formation kinetics in Mg-2Ce since values for *H* diffusivity in pure Mg were unavailable. It was stated that for the given crack velocity insignificant *H* diffusion would occur for $D < 2 \times 10^{-7}$ cm^2/s. However, Makar et al.[83] postulated that the *H* diffusivity might be as large as 10^{-6} cm^2/s.

Meletis and Hochman[72] reported that crack initiation and propagation for pure Mg in a chloride-chromate solution was accompanied by *H* evolution. Using electron channeling pattern analysis and SEM photogrammetry they showed that cracks propagated primarily by cleavage on $\{2\bar{2}03\}$ planes as evidenced by parallel facets. These facets were separated by steps also on $\{2\bar{2}03\}$ planes. The authors proposed that cleavage occurs by reduction in surface energy of $\{2\bar{2}03\}$ planes by HE resulting from preferential *H* accumulation or hydride formation on these planes. *H* may be absorbed from the solution at the crack tip or transported to the region by dislocation motion.

Bursle and Pugh[14] also concluded that cracking in Mg-Al occurs by discontinuous cleavage induced by HE. They rejected the adsorption model (reduction of metal inter-atomic bond strength at the crack tip by the interacting of absorbed ions) on the basis that adsorption would only affect a few atomic layers ahead of the crack tip, and therefore it would not cause discontinuous crack propagation involving the distances between crack arrest markings observed by SEM. Adsorption induced propagation would be macroscopically continuous at a rate determined by the transport of ions to the crack tip. Dealloying models were also rejected on the basis that solutions that cause dealloying are not usually associated with TGSCC and there has been no correlation reported between dealloying and cleavage.

Bursle and Pugh observed a 1 μm layer of brittle Mg hydride (MgH_2) on the cleavage fracture surfaces of Mg-Al specimens, contradicting Lynch and Trevena.[71] That this compound was not apparent on external or ductile fracture surfaces suggests that hydride formation was stress-induced. The authors also proposed that the $\{31\bar{4}0\}$ planes, determined by the two surface trace technique and a photogrammetric method, to be the orientation of the cleavage facets, may also be the habit or cleavage plane of the hydride. These factors lead to the proposal that hydrogen embrittlement as illustrated in Figure 2 was the dominant mechanism for crack propagation.

5. Open Issues

5.1. Mechanisms

The most recent mechanistic studies have established the main components important for the propagation of SCC. The work of Pugh and co-workers[14,86,88,89,121] has provided convincing evidence for a brittle cleavage type mechanism involving *H*. Particularly noteworthy are the stepped and facetted interlocking fracture surfaces. In contrast, the fractogra-

phy of Lynch and Trevena[71] indicates some plasticity, particularly at higher loading rates and faster crack velocities. The slow strain rate testing of both Ebtehaj et al.[107] and Stampella et al.[75] indicate a mechanism involving strain induced film rupture leading to corrosion and *H* production, with crack advance due to *H*. Makar et al.[83] confirmed the fractography previously observed, the importance of strain rate and *H*, but they propose a brittle hydride model.

Thus, there is agreement that *H* is part of the SCC propagation mechanism but disagreement on the role that *H* plays. Moreover, as pointed out by Makar et al.[83] the diffusion coefficient for *H* in Mg has not been measured. Thus, there is no good data on *H* transport that is needed for an evaluation of the role that *H* plays. The mechanistic considerations of Makar et al.[83] suggest that the intrinsic diffusion coefficient of *H* in Mg should be between about 10^{-7} to 10^{-5} cm^2/s at 22–24 °C. The only actual measurement related to *H* diffusion in Mg that was found was that in the review by Fisher,[125] which provides a summary of a study by Spatz et al.[126] that suggests a diffusion coefficient of 1.1×10^{-20} m^2/s.

Concerning the key aspects of the environment, the mechanistic hypothesis that emerges from the prior work is that SCC is associated with environmental conditions leading to the local breakdown of a partially protective surface film. Film breakdown can be caused by the environment, e.g. pitting by chloride ions. However, the facts that SCC occurs for (1) pure Mg in a dilute sulphate solution and (2) Mg alloys (AZ91, AM60, AS41, ZK60A-T5) in distilled water, indicates that film breakdown may also be a role of the loading. The role of the film is also consistent with it acting as a barrier preventing hydrogen ingress into the metallic Mg alloy, the hydrogen being produced as part of the Mg corrosion reaction.

5.2. Stress

The prior work has indicated that the loading causes SCC above a threshold (threshold stress or threshold stress intensity factor). Above the threshold, SCC can be characterised by the crack propagation velocity. Moreover, the threshold and the crack velocity are both influenced by both the environment as well as by the rate of loading. There are too many variables for an empirical characterisation, and hence a mechanistic approach is required.

5.3. Environment

What are the critical parameters that typify an SCC environment? As *H* appears part of the SCC mechanism, is it possible to develop a measure of *H* activity to characterise the conditions causing SCC?

5.4. Probable Service Environments

The following environments will most likely encompass 80-90 % of Mg applications for the immediate future:

(i) Moist air (with intermittent wetting and drying). This represents normal atmospheric exposure.

(ii) Moist air + road salt (containing particularly chloride ions). A typical example might be a magnesium engine block in northern America or Europe where significant quantities of road salt are used.

(iii) Case (ii) in marine locations, i.e. with the presence of sea salt.

(iv) Engine coolant operated in sub-zero external conditions.

Case (iv) is particularly interesting to Mg alloy producers and also to the automobile industry. It presents interesting corrosion issues. The engine coolant typically contains the following ingredients: (1) water, (2) an antifreeze agent such as ethylene glycol, and (3) inhibitors. Inorganic inhibitors in use include phosphate, nitrate, silicate and aluminate ions.

5.5. Alloy

There is little published SCC research on cast Mg alloys, particularly modern and experimental alloys. This is in contrast to the considerable research on the SCC of wrought Mg alloys during the 60s, 70s and 80s and on rapidly solidified Mg alloys in the early 90s, which was prompted by the needs of the aerospace and defence industries. Early reviews[68,127] in 1966 reported that alloying additions such as Al and Zn to wrought Mg alloys promoted SCC; thus wrought AZxx alloys were susceptible to SCC for intermittent exposure to 0.01 % NaCl and to the weather (i.e. humid air with intermittent wetting and drying), whereas M1 and (the then existing) Zr containing alloys were reported to be free of SCC. Subsequent studies, summarised above and in Table 2, have mostly concentrated on pure Mg or Mg-Al alloys, but SCC has been shown for a number of Al free alloys. Table 4 provides a summary of values of SCC threshold stress extracted from Table 2.

This prior work on pure Mg, Mg-Al alloys and Zr containing alloys showed that SCC is a significant issue, and that SCC can occur for a load condition equivalent to 40-50 % of the yield stress for many combinations of alloy + environment. This work is in contrast to the earlier reports and to the perception of SCC resistance of pure Mg and Mg-Mn alloys. Clearly this early work needs to be checked, particularly for modern cast alloys.

Since the prior research indicates that all Mg alloys are likely to be more or less susceptible, guidelines are needed to ensure safe application of Mg alloys in service. It would seem that an urgent task would be to delineate safe operational limits for common alloys in likely service environments. A way forward may be the measurements of the threshold

Table 4. Values of SCC threshold stress for common Mg Alloys from Table 2.

Alloy, Environment	σ_{SCC}
HP Mg, 0.5%KHF_2	60%YS
Mg2Mn, 0.5%KHF_2	50%YS
MgMnCe, air, 0.001N NaCl, 0.01Na_2SO_4	85%YS
ZK60A-T5, rural atmosphere	50%YS
QE22, rural atmosphere	70–80%YS
HK31, rural atmosphere	70–80%YS
HM21, rural atmosphere	70–80%YS
HP AM60, distilled water	40–50%YS
HP AS41, distilled water	40–50%YS
AZ31, rural atmosphere	40%YS
AZ61, costal atmosphere	50%YS
AZ63-T6, rural atmosphere	60%YS
HP AZ91, distilled water	40–50%YS

stress and threshold stress intensity factor, see Figure 14, for the common commercial alloys in the environments enunciated in Section 5.4.

Table 4 indicates that it would be conservative to assume that the threshold stress was ~40–50 %YS, unless there is convincing data showing otherwise for the particular alloy + environment combination. It would be prudent to apply this recommendation for the common Mg alloys in the environments enunciated above in Section 5.4.

5.6. Understanding the Environment Influence

It is generally known that SCC susceptibility is specific to alloy-environment combinations, many of which have not previously been investigated. Reports on the susceptibility of Mg alloys in solutions containing carbonate, fluoride, nitrate, silicate and phosphate ions are generally ambiguous, and a detailed mechanistic understanding of their influences is needed. The work of Ebtehaj et al.[107] indicated interdependent influences of solution composition, electrochemical potential and strain rate. This implies that empirical development of such an understanding would require evaluation of a large number of combinations of environmental parameters. Basic trends in the influence of solution pH and temperature on SCC susceptibility have been reported; however, a mechanistic understanding of these influences is also required.

Environmental influences are generally characterized according to SCC thresholds, time-preceding-cracking, steady-state crack propagation velocity and total time-to-failure. The coupling of the SCC stages (crack initiation, steady-state crack propagation and ductile fracture) by incorporating average crack velocities into numerical models has been a limiting factor in many previous works. Makar et al.[83] measured crack velocity by dividing the stress corrosion crack length or total crack length by time-to-failure; however, considerable separation of these two parameters was observed, particularly at high strain rates. More accurate determination of these parameters requires measurement of crack extension with respect to time. This has previously been achieved through the use of traveling microscopes,[105,121] and by the use of potential drop techniques.[46,48,130]

There is an obvious need to explain trends in environmental susceptibility of Mg alloys with respect to an irrefutable HE model. Currently, there is much conjecture regarding the validity of several models (see Sec. 5.1). This conflict may be partly attributed to inaccurate numerical modeling of the steady-state crack propagation velocity, resulting from uncertainty regarding the *H* diffusion coefficient, or that the preeminent mechanism is specific to the environment-alloy combination or conditions of applied stress and strain. There is a need to investigate the latter possibility by comparing fracture surfaces, *H* activity and SCC parameters for different systems and conditions. Such work would represent a significant development in the understanding of SCC in Mg alloys.

Chakrapani and Pugh[89] proposed that HE occurs by brittle hydride formation, and showed that the *H* concentration of Mg-7.5Al specimens stressed in NaCl-K_2CrO_4 solution progressively increased with time. However, if MgH_2 is stable at room temperature, as proposed by Stampella et al.[75] the hydride model is contradicted by Chakrapani and Pugh's own reports that *H* effects were reversed by vacuum annealing. Adding to the confusion is the report by Bursle and Pugh[14] that MgH_2 was present on the fracture surfaces of Mg-7.5Al specimens stressed in the NaCl-K_2CrO_4 solution. This dispute indicates a critical void in the existing knowledge; consequently, there is a need to determine which environmental and loading conditions, if any, promote the formation of MgH_2 on crystallographic planes.

Lynch and Trevena[71] proposed that for large-grained pure Mg in a NaCl-K_2CrO_4 solution, HE occurs by AIDE, in which adsorbed *H* atoms weaken interatomic bonds at crack tips thereby facilitating dislocation nucleation and crack coalescence. This was supported by fractographic comparisons between LME and SCC specimens for crack velocities up to $\sim 50 \times 10^{-3}$ m/s, at which insufficient time is available for diffusion to occur. However, it was proposed that at lower velocities (as low as $\sim 10^{-8}$ m/s) some diffusion would occur since adsorption would be partly inhibited by film formation, as evidenced by a slightly different fracture surface topography. Bursle and Pugh[14] speculated that for SCC of Mg-7.5Al alloy in a NaCl-K_2CrO_4 solution, adsorption would only penetrate a few atomic layers ahead of the crack tip; therefore, it could not explain the observed distances between crack arrest markings. Consequently, there exists a need to quantify *H* penetration according to the various mechanisms and correlate this with fracture surface topography. This would help to resolve disputes regarding the HE mechanisms.

6. SCC Testing and Research

6.1. Approach

Previous service failure data of Mg alloys are not so numerous, and, in many cases, access to this data is somewhat difficult. Accelerated tests of the bare, unprotected metal are useful to establish a minimum required basis of performance, whilst prediction of service life requires evaluation of the coatings and selection of maintenance procedures. Corrosion rates tend generally to decrease as the electrolyte becomes saturated with Mg ions, depending on the quality of the surface film and the pH shift. Consequently, it is important to consider solution pH, flow rates and ratio of area of metal surface to volume of solution.

The most common approaches employed to achieve testing objectives in SCC are the use of high stresses, slow continuous straining, precracked specimens, a concentration of species in the test environment higher than in the service environment, increased temperature, and electrochemical stimulation. Corrosion testing can help in the development of new alloys that can be less expensive, and offer longer, more safe and more efficient service.[66]

The objectives of SCC testing is either (1) to provide data that underpin service use, or (2) to elucidate the SCC phenomena and SCC mechanism(s). When underpinning service use, it is important to ensure that the laboratory studies reflect the conditions in service, particularly that the SCC mechanism examined in the laboratory is the same as that potentially encountered in service. Detailed comparison of fractography can be helpful in this regard.[39,41]As discussed previously, there is an urgent need to characterise SCC for common and experimental alloys in likely service environments as discussed in Section 5.4; furthermore, the following four parameters can be used to characterise SCC for a particular alloy + environment: the time to SCC initiation, the threshold stress, σ_{SCC}, the threshold stress intensity factor, K_{1SCC}, and the steady state stress corrosion crack velocity.

6.2. Specimens and Loading

Commonly used types of plain specimens have included bend-beam specimens, C-ring specimens, O-ring specimens, tension specimens and tuning fork specimens. Plastic strain specimens, residual stress specimens, static loading of precracked specimens and slow-strain-rate testing have all been used. The specimens can be subjected to various loading conditions involving constant load, constant strain, or monotonically increasing strain or stress to total failure. Other tests have included cyclic loading as well as slow straining over a limited stress range.

As discussed in Section 3.2.2, constant load tests have been reported, in some particular circumstances, to be more severe than constant displacement tests[16,95] in that it has been found that SCC has occurred in constant load tests whereas the constant displacement tests have indicated no SCC susceptibility.[50]

Threshold stresses have typically been measured using tensile loaded smooth samples,[15,76,84,90,100] and slow loading accompanied by a potential drop technique.[46,48,49] The potential drop technique measures crack initiation and monitors crack propagation by the change of electrical potential (resistance) of a specimen through which flows a constant current, typically 5–20 *A*. The resistance of the specimen increases as the cross-section is decreased by crack propagation. The potential drop technique has been used to identify crack initiation, and hence has been used in the measurement of the threshold stress.

For testing cylindrical tensile specimens, the solutions have been contained in cylindrical tubes closed at each end with rubber stoppers and with facilities for measuring or controlling the potential with respect to an external reference electrode, often a saturated calomel electrode. Note the possible importance of partial immersion as shown by the work of Miller,[84] who observed that the SCC occurred always associated with the solution-air interface for partially immersed specimens. For tests on bar specimens, the test solution have been contained in the region of the notch by pieces of adhesive tape attached to opposite sides of the specimen, the solution level in the notch being below the position of attachment of the COD gauge arms.

The threshold stress intensity factor and the stress corrosion crack velocity can be investigated with pre-cracked fracture mechanism type specimens.[128,129] Crack initiation and crack growth can be monitored using potential drop techniques.[130]

6.3. Testing Environments

SCC testing can be divided into those conducted in natural environments, such as atmospheric exposure tests and seawater immersion tests, and those which are conducted under laboratory conditions. Externally applied loads are easier to evaluate and to control, but residual stresses have been responsible for SCC failures in service. Laboratory tests may be quick and are useful in encouraging conservative design of magnesium alloy structures, but it is important to ensure that laboratory tests are developed that do simulate service.

6.3.1. Natural Environments

Atmospheric exposures have been used in the SCC testing of Mg alloys.[15,100] A principal disadvantage of such tests is the comparatively long time required for their completion. In the investigation of experimental alloys, thermal treatments, and other means of preventing SCC in Mg alloys, accelerated tests are required that will give results in comparatively short times. Furthermore, applications of Mg alloys in service are such that it is important to consider environments other

than just exposure to the atmosphere, as discussed in Section 5.4.

6.3.2. Immersion, Alternating Immersion and Spray Testing

Alternate salt immersion and salt spray testing has been standardised by ASTM G 44-88 and ASTM B-117-95.[131] However, it seems that some of these generally accepted tests are somewhat severe for uncoated Mg alloys. The solution of 3.5 % NaCl, pH 6.5, is recommended in these tests, however, this provides high corrosion rates and is unlikely to be representative of many of the service environments for Mg alloys.

Popular solutions for SCC testing of Mg alloys have been those containing chloride and chromates.[15,107] A major problem with these is that the "accelerated test solution" has been less severe than exposure to the atmosphere[15] (see Tab. 2), so it is important with these solutions to consider carefully the concentration and the chloride/chromate ratio[107] (see Fig. 21). Figure 21 indicates that an interesting testing solution might be 2 g/L NaCl + 2 g/L K_2CrO_4. This solution might have sufficient chloride for depassivation and SCC, sufficient chromate to give low rates of general corrosion, and may provide SCC susceptibility over a wide range of applied strain rates.

Considering the likely service environments, consideration might be given to the use of relatively dilute solutions, like distilled water (used particularly by Miller[84]) and de-aerated, aqueous 10^{-3} *M* Na_2SO_4 solution with the pH adjusted to 10.0 by additions of sodium hydroxide,[75] and solutions to simulate possible SCC processes in auto engine coolants.

Use of a solution in a SCC testing/research program is relatively straightforward and useful for elucidating the SCC mechanism. Particularly in mechanistic studies, it is important to be able to fully control all variables of importance. However, it is also useful to remember that Miller[84] found that the SCC of AZ91, AM60 and AS41 was invariably associated with the solution-air interface for SCC testing using partially immersed specimens. This type of situation would be expected to be particularly important in service, e.g. for auto applications subjected to road splash.

6.4. Planned Research

Future work at The University of Queensland (UQ) and GKSS is, inter alia, planned to address the issue of understanding the influence of the environment, as shown schematically in Figure 40. This research is planned to focus on TGSCC of AZ91 and ZE41 cast alloys in solutions containing ethylene glycol and chloride, sulphate, carbonate, fluoride, chromate, nitrate, silicate and phosphate ions. These alloy-environment combinations are particularly relevant to the service of cast Mg alloys in automotive applications. Benchmark tests will be conducted on pure Mg in the above environments, and on the commercial cast Mg alloys in distilled water and inert environments. The influence of solution composition, electrochemical potential, pH and temperature will be investigated. The primary objective is to develop a mechanistic understanding of the influences of various environmental parameters on TGSCC susceptibility of cast Mg alloys.

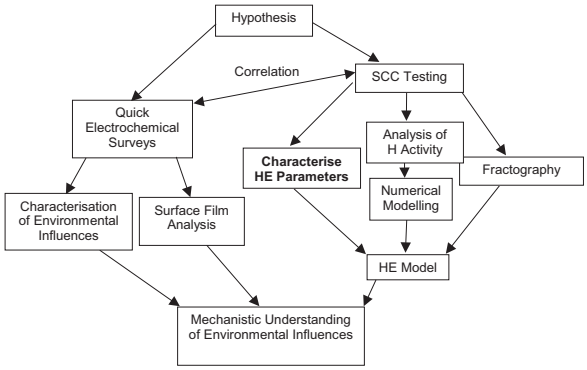

Fig. 40. Schematic of proposed research on environmental influences for Mg alloys.

7. Recommendations to Avoid SCC

The prevention of SCC for Mg alloys is a delicate subject. The general principle for SCC prevention is to avoid loading a susceptible alloy above a critical stress during exposure to a SCC producing environment. SCC prevention is a serious task for Mg alloys, since SCC can be produced in distilled water for applied stresses above 50 % YS. There is inadequate data, partly because the use of Mg alloys as a structural material is relatively recent and reported service failures are not numerous. Research is underway to understand the SCC mechanisms. Evaluation of the SCC of Mg alloys is also in progress and is urgently needed to supply appropriate schemes for SCC prevention. However, the authors wish to offer some general guidelines that should be handled by the Engineer very carefully for every practical situation.

7.1. Conception and Design

This is a general trend in SCC prevention to start with a design that avoids concentration of stresses at the start, or during use, or through increasing susceptibility to different forms of degradation in service, especially localised corrosion, galvanic corrosion, (corrosion) fatigue and erosion-corrosion.

7.2. Service Environment

SCC is expected to not be an issue for dry atmospheres provided the relative humidity is less than 95 % and provided that there are no crevices. For crevices, capillary condensation can cause the formation of a liquid in the crevices at lower values of relative humidity. It would be prudent to fill crevices with a corrosion-inhibited putty. Furthermore, crevices

are part of the microstructure of diecast alloys, which might be part of the reason that Miller[84] measured threshold valued of 40-50 %YS for AZ91, AM60 and AS41 in distilled water.

Cathodic polarization may reduce, or even prevent SCC of magnesium alloys in aqueous solutions.

7.3. Alloy Selection

Table 2 indicates that SCC occurs for many alloy + environment combination and Table 3 provides only some references to alloy + environment combinations where there is information regarding SCC resistance. Moreover, the data of Table 3 needs to be approached with the appropriate degree of critical evaluation. The one situation that does seem to merit more attention is the use of Mg-Mn alloys, including the use of Mg-2Mn as cladding for higher strength Mg alloys.

7.4. Service Loading

The total stress in service (stress from the service loading + the fabrication stress + the residual stress) should be below the threshold level[132] which, in the absence of other data could be estimated from Table 2 to be ~40–50 % of the tensile yield strength.

Bolted or riveted joints can also produce high local stresses that can cause SCC, so that attention should be given to joint design and construction. Examples include the use of preformed parts, avoiding over-torquing of bolts, and providing adequate spacing and edge margins for rivets.[132]

Tensile residual stresses from welding can be particularly dangerous and a low temperature thermal stress relief treatment has been recommended for welded assemblies.[74]

Inserts with a wall thickness greater than 1.25 mm (0.050 in.) should be preheated before casting, because cast-in inserts may cause SCC due to local residual stresses created in the surrounding magnesium.[132]

Shot peening, surface rolling, abrasion and mechanical processes, that create compressive surface residual stresses, may also be effective in increasing SCC resistance.[74] Please do note that shot peening must be optimised for Mg alloys; in particular use of steel shot is unacceptable as it leads to surface contamination with Fe and concomitantly high corrosion rates.

Scully[114] reports that stress relieving at low temperatures is commonly used to lower susceptibility in Mg alloys, e.g. 8 h at 125 °C for Mg-6.5Al-1Zn-0.3Mn, since higher temperatures tend to lower the yield point.

7.5. Anodizing etc.

The prime function of anodising, other coatings, surface treatments and inhibitors, is to prevent the Mg alloy from contacting the environment. There would be no SCC if there were no contact with the environment. Breaks or holidays in the coating could lead to SCC. Scully[114] reports that surface oxidation followed by anodising has been reported to increase SCC life. Coatings have been shown to extend life, but not to totally prevent SCC, with breaks in the coating reducing protection.[74] In another laboratory study, an inorganic coating was found to accelerate SCC of a SCC resistant alloy.[112]

7.6. Inspection and Maintenance

There should be appropriate inspection and maintenance programs to avoid SCC and precursors, for example a concentration of stresses by localised corrosion. For corrosion protection by protective coatings, routine maintenance is essential since scratches could create favourable sites for initiation of SCC.

Received: March 18, 2005
Final version: April 25, 2005

[1] G. Song, A. Atrens, *Adv. Eng. Mater.* **1999**, *1*, 11.
[2] G. L. Song, A. Atrens, *Adv. Eng. Mater.* **2003**, *5*, 837.
[3] E. Ghali, *Magnesium and Magnesium Alloys*, in *Uhlig's Corrosion Handbook*, Wiley-Interscience, **2000**, 793.
[4] Y. Kojima et al eds, *Materials Science Forum* **2003**, *419–422*, 1.
[5] G. S. Cole, *Materials Science Forum* **2003**, 419-422, 43.
[6] International Magnesium Association, *2002-year end report*, www.intlmag.org.
[7] E. Ghali, W. Dietzel, K. U. Kainer, *Journal of Materials and Performance*, ASM, **2004**, *13*, 7.
[8] E. Ghali, W. Dietzel, K. U. Kainer, *Journal of Materials and Performance*, ASM, **2004**, *13*, 517.
[9] *ASM Handbook, Vol 13, "Corrosion"* ASM International, fourth printing **1992**.
[10] I. J. Polmear, *Light alloys: metallurgy of the light metals*, Arnold, London **1995**.
[11] A. Atrens, Z. F. Wang, *Materials Forum*, **1995**, *19*, 9.
[12] W. Dietzel, *Encyclopedia of Materials: Science and Technology*, Elsevier Science Ltd., Amsterdam, **2001**, 8883.
[13] R. H. Jones, R. E. Ricker, in *Stress Corrosion Cracking: Materials Performance and Evaluation*, ASM International, USA, **1992**, 1.
[14] A. J. Bursle, E. N. Pugh, in *Mechanisms of Environment Sensitive Cracking of Materials*, Materials Society (London), **1977**, 471.
[15] W. S. Loose, H. A. Barbian, in *Symposium on Stress Corrosion Cracking of Metals*, American Society for Testing Materials, USA, **1945**, 273.
[16] W. K. Miller, in *Stress Corrosion Cracking: Materials Performance and Evaluation*, ASM International, USA, **1992**, 251.

[17] M. O. Speidel, P. M. Fourt, in *Stress Corrosion Cracking and Hydrogen Embrittlement of Iron Base Alloys*, NACE, Houston, USA, **1977**, 57.
[18] P Lyon, Magnesium Electron UK, *private communication* Feb **2001**.
[19] C Blawert, N Hort, K. U. Kainer, *Trans Indian Inst Met* **2004**, *57*, 397.
[20] A. Atrens, *Adv. Eng. Mater.* **2004, 6**, 83.
[21] G. Song, A. Atrens, in *Corrosion and Environmental Degradation of Materials: Volume 19 of the Series: Materials Science and Technology*, Wiley-VCH Verlag GmbH **2000**.
[22] G. Song, A. Atrens, S. StJohn, J. Nairn, Y. Lang, *Corrosion Science* **1997**, *39*, 855.
[23] G. Song, A. Atrens, D. StJohn, *Corrosion Science* **1997**, *39*, 1981.
[24] G. Song, A. Atrens, X Wu, B. Zhang, *Corrosion Science* **1998**, *40*, 1769.
[25] G. Song, A. Atrens, M. Dargusch, *Corrosion Science* **1999**, *41*, 249.
[26] G. Song, preprint of paper presented "Corrosion Science in the 21st century" UMIST 7–11 July, 2003, *Journal of Corrosion Science and Engineering*.
[27] G. Song, D. H. StJohn, *Journal of Light Metals* **2002**, *2*, 1.
[28] G. Song, A. Atrens, D. H. StJohn, in J Hryn ed, *Magnesium Technology 2001*, New Orleans, TMS **2001**, 255.
[29] G. Song, A. L. Bowles, D. H. StJohn, *Materials Science and Engineering*, **2004**, *A 366*, 74.
[30] G. Song, A. Atrens, *International conference on magnesium alloys and their applications*, Wolfsburg **1998**, 415.
[31] G. Song , D. H. StJohn, *J Light Metals* **2002**, *2*, 1.
[32] G. Song, B. Jonhannesson, Sarath Hapugoda, D. H. StJohn, *Corrosion Science*, **2004**, *46*, 955.
[33] J. X. Jia, G. Song, A. Atrens, D. StJohn, J. Baynham, G. Chandler, *Materials and Corrosion*, **2004**, **55**, 845
[34] J. J. Jia, G. Song, A. Atrens, *Materials and Corrosion* **2005**, *56*, 259.
[35] Zhiming Shi, Guanglin Song, Andrej Atrens, *Surface and coating Technology*, submitted for publication.
[36] A. Atrens, J. Q. Wang, K. Stiller, H. O. Andren, *Corrosion Science* **2005**, *47*, accepted for publication.
[37] A. Atrens, S. Humphrey, J. J. P. Piper, J. Q. Wang, *Proceedings of CORROSION/2004 Research Topical Symposium: Corrosion Modelling for Assessing the Condition of Oil and Gas Pipelines*, Chair F King, Vice Chair J Beavers, NACE Press, Houston, **2004**, 275.
[38] J. Q. Wang, A. Atrens, *Engineering Failure Analysis*, **2004**, *11*, 3.
[39] E. Gamboa, A. Atrens, *Engineering Failure Analysis*, **2005**, *12*, 201.
[40] J. Wang, A. Atrens, *Corrosion Science* **2003**, *45*, 2199.
[41] E. Gamboa, A. Atrens, *Engineering Failure Analysis* **2003**, *10*, 521.
[42] J. Q. Wang, A. Atrens, D. R. Cousens, P. M. Kelly, C. Nockolds, S. Bulcock, *Acta Materialia*. **1998**, *46*, 5677.
[43] A. Oehlert, A. Atrens, *J. Materials Science* **1998**, *33*, 775.
[44] A. Oehlert, A. Atrens, *J. Materials Science* **1997**, *32*, 6519.
[45] A. Oehlert, A. Atrens, *Corrosion Science*, **1996**, *38*, 1159.
[46] Z. F. Wang, A. Atrens, *Metallurgical and Materials Transactions*, **1996**, 27A, 2686.
[47] A. Oehlert, A. Atrens, *Acta Metallurgica et Materialia*, **1994**, *42*, 1493.
[48] A. Atrens, C. C. Brosnan, S. Ramamurthy, A. Oehlert, I. O. Smith, *Measurement Science and Technology*, **1993, 4**, 1281
[49] S. Ramamurthy, A. Atrens, *Corrosion Science*, **1993**, *34*, 1385.
[50] R. M. Rieck, A. Atrens, I. O. Smith, *Met Trans*, **1989, 20A**, 889
[51] R. G. Song, W. Dietzel, B. J. Zhang, W. J. Liu, M. K. Tseng, A. Atrens, *Acta Materialia* **2004**, *52*, 4727.
[52] R. M. Rieck, A. Atrens, I. O. Smith, *Materials Science and Technology*, **1986**, *2*, 1066.
[53] C. D. Cann, A. Atrens, *J. Nuclear Materials*, **1980**, *88*, 42
[54] A. Atrens, D. Mezzanotte, N. F. Fiore, M. A. Genshaw, *Corrosion Science* **1980**, ***20***, 673.
[55] A. Atrens, J. J. Bellina, N. F. Fiore, R. J. Coyle, *The Metal Science of Stainless Steels*, WE Collings and HW King, Editors, TMS-AIME, **1978**, 54.
[56] A. Atrens, H. Meyer, G. Faber, K. Schneider, in *Corrosion in Power Generating Equipment*, Editors, Plenum, **1984**, 299.
[57] A. Atrens, W. Hoffelner, T. W. Duering, J. Allison, *Scripta Metallurgica* **1983**, *17*, 601.
[58] I. G. Ritchie, A. Atrens, *J. Nuclear Materials* **1977**, *67*, 254.
[59] S. Jin, A. Atrens, *Applied Physics A* **1987**, *42*, 149.
[60] A. S. Lim, A. Atrens, *Applied Physics A* **1992**, *54*, 500.
[61] A. S. Lim, A. Atrens, *Applied Physics A* **1990**, *51*, 411.
[62] Guanglin Song, Andrej Atrens, Ying Li, Bo Zhang, *Proceedings of Corrosion and Prevention-97*, Australiasian Corrosion Association Inc., **1997**, 38.
[63] M. Pourbaix, *Atlas of Electrochemical Equilibria in Aqueous Solutions*, NACE Houston TX, CEBELCOR Brussels **1974**.
[64] D. A. Jones, *Principles and Prevention of Corrosion*, Prentice Hall **1996**.
[65] J. D. Hanawalt, C. E. Nelson, J. A. Peloubet, *Trans. Am. Inst. Mining Met.Eng.* **1942**, *147*, 273.
[66] J. E. Hillis, Reece Wilton Murray, *SDCE 14th International Die Casting Congress and Exposition, Toronto,* **1987**, *Paper No. G-T87-003.*
[67] A. L. Olsen, Translation of Paper presented at the *"Deutscher Verband fü Materialforschung u. Prüfung e.v." Bauteil'91. Berlin*, **1991**, *1–21.*
[68] E. F. Emley, *Principles of Magnesium Technology*, Pergamon Press, **1966**, Chapter XX.
[69] D. S. Tawil, *NACE90 Las Vegas*, **1990**, Paper no 90445.
[70] K. Nisancioglu, O. Lunder, T. Aune, *Proc 47th World Magnesium Conference*, Cannes IMA, **1990**, 43.
[71] S. P. Lynch, P. Trevena, *Corrosion* **1988**, *44*, 113.
[72] E. I. Meletis, R. F. Hochman, *Corrosion* **1984**, *40*, 39.
[73] ASM Specialty Handbook: *Magnesium and Magnesium Alloys*, ASM International, USA **1999**, 211.

[74] M. A. Timonova, *Intercrystalline Corrosion and Corrosion of Metals Under Stress*, Ed. I.A. Levin, Great Britain, **1962**, 263.
[75] R. S. Stampella, R. P. M. Procter, V. Ashworth, *Corrosion Science* **1984**, *24*, 325.
[76] L. Fairman, H. J. Bray, *Corrosion Science* **1971**, *11*, 533.
[77] Datasheet: *AZ91 Magnesium Alloys*, Hydro Magnesium, Belgium, 2004.
[78] Matweb: *Material Property Data*, 2004, http://www.matweb.com.
[79] R. S. Busk, *Magnesium Products Design* M. Dekker, USA, **1986**, 256.
[80] D. K. Priest, F. H. Beck, M. G. Fontana, *Transactions of the American Society for Metals*, **1955**, *47*, 473.
[81] M. A. Pelensky, A. Gallaccio, *Stress Corrosion Testing, STP425*, ASTM **1967**, 107.
[82] H. L. Logan, H. Hessing, *Journal of Research of the National Bureau of Standards* **1950**, 44, 233.
[83] G. L. Makar, J. Kruger, K. Sieradzki, *Corrosion Science* **1993**, *34*, 1311.
[84] W. K. Miller, *Mat Res Soc Symp Proc* **1988**, *125*, 253.
[85] W. R. Wearmouth, G. P. Dean, R. N. Parkins, *Corrosion* **1973**, *29*, 251.
[86] D. G. Chakrapani, E. N. Pugh, *Metallurgical Transactions* **1975**, *6A*, 1155.
[87] G. Oryall, D. Tromans, *Corrosion* **1971**, *27*, 334.
[88] D. G. Chakrapani, E. N. Pugh, *Corrosion* **1975**, *31*, 247.
[89] D. G. Chakrapani, E. N. Pugh, *Metallurgical Transactions* **1976**, *7A*, 173.
[90] E. C. W. Perryman, *Journal of the Institute of Metals* **1951**, *78*, 621.
[91] T. Nozaki, S. Hanaki, M. Yamashita, H. Uchida, *Proceedings of the 13th Asian-Pacific Corrosion Control Conference*, Osaka, **2003**, K-15.
[92] L. Fairman, J. M. West, *Corrosion Science* **1965**, *5*, 711.
[93] A. Moccari, C. R. Shastry, Journal of Materials Technology (Zeitschrift für Werkstofftechnik), **1979**, 10, 119.
[94] L. Fairman, H. J. Bray, *British Corrosion Journal* **1971**, *6*, 170.
[95] W. M. Pardue, F. H. Beck, M. G. Fontana, *Transactions of the American Society for Metals* **1961**, *54*, 539.
[96] D. A. Jones, *Principles and Prevention of Corrosion*, Macmillan Publishing Company, USA, **1992.**
[97] N. D. Tomashov, V. N. Modestova, *Intercrystalline Corrosion and Corrosion of Metals Under Stress*, Great Britain, **1962**, 251.
[98] R. Heidenrich, C. H. Gerould, F. E. McNulty, *Transactions of the AIME*, **1946**, *166*, 15.
[99] L. L. Rokhlin, *Magnesium Alloys Containing Rare Earth Metals*, Taylor and Francis, UK **2003**, 221.
[100] Exterior Stress Corrosion Resistance of Commercial Magnesium Alloys, Report Mt 19622, Dow Chemical USA, **1966.**
[101] R. I. Stephens, C. D. Schrader, D. L. Goodenberger, K. B. Lease, V. V. Ogarevic, S. N. Perov, *Society of Automotive Engineers, No. 930752*, USA, **1993.**
[102] S. Mathieu, C. Rapin, J. Hazan, P. Steinmetz, *Corrosion Science* **2002**, *44*, 2737.
[103] M. A. Timonova, L. I. D'yalchenko, Yu. M. Dolzhanskii, M. B. Al'tman, N. V. Sakharova, A. A. Blyablin, *Protection of Metals* **1983**, *19*, 99.
[104] R. B. Mears, R. H. Brown, E. H. Dix, in *Symposium on Stress-Corrosion Cracking of Metals*, American Society for Testing Materials **1945**, 323.
[105] M. O. Speidel, M. J. Blackburn, T. R. Beck, J. A. Feeney, *Corrosion Fatigue: Chemistry, Mechanics and Microstructure*, NACE-2 1**972**, 324.
[106] J. C. Kiszka, *Materials Protection* **1965**, *4*, 28
[107] K. Ebtehaj, D. Hardie, R. N. Parkins, *Corrosion Science* **1993**, ***28***, 811.
[108] Z. L. Wei, Q. R. Chen, Z. C. Guo, L Yang, N. X. Xiu, Y. W. Huang, in *Magnesium – Proceedings of the 6th International Conference Magnesium Alloys and Their Applications*, KU Kainer ed, Wiley-VCH **2004**, 649.
[109] T. J. Marrow, A. B. Ahmad, I. N. Kahn, S. M. A Sim, S. Torkamani, *Mat Sci and Eng A* **2004**, *387–389*, 419.
[110] L. Fairman, H. J. Bray, *Corrosion Science* **1971**, *11*, 533.
[111] R. P. Frankenthal, *Corrosion Science* **1967**, *7*, 61.
[112] V. B. Yakovlev, L. P. Trutneva, N. I. Isaev, G. Nemetch, *Protection of Metals* **1984**, *20*, 300.
[113] V. A. Marichev, S. A. Shipilov, *Soviet Materials Science* **1986**, *33*, 240.
[114] J. C. Scully, in *Corrosion*, Butterworth Heinemann, **1993**, *8*:115–142.
[115] H. L Logan, *Journal of Research of the National Bureau of Standards* **1958**, *61*, 503.
[116] G. F. Sager, R. H. Brown, R. B. Mears, *Symposium on Stress-Corrosion Cracking of Metals*, ASTM, **1945**, 267.
[117] W. S. Loose, *Magnesium*, ASM Ceveland Ohio USA, **1956**, 173.
[118] V. V. Romanov, Intercrystalline Corrosion and Corrosion of Metals Under Stress, Great Britain **1962**, 283.
[119] F. Meller, M. Metzger, U.S.N.A.C.A. Tech Note No 4019 (19857).
[120] H. L. Logan, *Journal of Research of the National Bureau of Standards* **1952**, *48*, 99.
[121] E. H. Pugh, J. A. S. Green, P. W. Slattery, *Fracture 1969: The Proceedings of the Second International Conference on Fracture*, Chapman and Hall Ltd, London **1969**, 387.
[122] H. W. Pickering, P. R. Swann, *Corrosion* **1963**, ***19***, 373.
[123] T. L. Anderson *Fracture Mechanics: Fundamentals and Applications* 2nd Edition, CRC Press, USA, **1992**.
[124] S. P. Lynch, *11th International Conference on Fracture*, **2005** paper p3885.
[125] D. J. Fisher, *Defect and Diffusion Forum* **1999**, *167–168*, 1.
[126] P. Spatz, H. A. Aerbisher, A. Krozer, L. Schlapbach, *Z für Physicaliscke Chemie* **1993**, *181*, 393.
[127] H. L. Logan, *The Stress Corrosion of Metals*, Wiley **1966**.
[128] M. O. Speidel, *Metall Trans* **1975**, *6A*, 631.
[129] W. Dietzel, Standardization of Rising Load/Rising Displacement SCC Testing, ASTM STP 1401 **2000**, 317.

ADVANCED ENGINEERING MATERIALS

[130] W. Dietzel, K.-H. Schwalbe, *Materialprüfung* **1986**, *28*, 368.
[131] ASTM G 44-88: Standard practice for evaluating Stress Corrosion Cracking resistance of metals and alloys by alternate immersion in 3.5 % sodium chloride solution **1988.**
[132] E. Groshart, *Magnesium, Part 1 – The Metal*, Metal Finishing **1985**, *83*, 17.

